AGU Books

A review of different modeling approaches used to simulate smoke transport and dispersion

Journal:	*AGU Books*
Manuscript ID	2021-Jun-CH-1395.R2
Wiley - Manuscript type:	Chapter
Date Submitted by the Author:	28-Jan-2022
Complete List of Authors:	Mallia, Derek; University of Utah, Dept. of Atmospheric Sciences Kochanski , Adam; San Jose State University, Department of Meteorology and Climate Science
Primary Index Term:	3390 - Wildland fire model < 3300 - ATMOSPHERIC PROCESSES
Index Term 1:	305 - Aerosols and particles (0345 , 4801 , 4906) < 300 - ATMOSPHERIC COMPOSITION AND STRUCTURE
Index Term 2:	3307 - Boundary layer processes < 3300 - ATMOSPHERIC PROCESSES
Index Term 3:	345 - Pollution: urban and regional (0305 , 0478 , 4251) < 300 - ATMOSPHERIC COMPOSITION AND STRUCTURE
Index Term 4:	3365 - Subgrid-scale (SGS) parameterization < 3300 - ATMOSPHERIC PROCESSES
Keywords:	Smoke modeling, Wildland fires, Air quality, Aerosols, Numerical weather prediction, Coupled fire-atmosphere interactions
Abstract:	A variety of smoke model frameworks are used to simulate smoke for research and forecast applications. Here, a comprehensive summary is provided which covers the many different smoke models that are available, while simultaneously highlighting some of the strengths and weaknesses of each model, along with the uncertainties surrounding each of these frameworks. This review also provides an in-depth discussion on coupled wildfire-atmosphere models, which is a relatively newer smoke modeling tool not previously discussed in other review papers. Key processes related to smoke transport and dispersion, such as the wildfire plume rise, are also discussed in length. This review wraps up with a discussion of future smoke modeling needs and potential new research directions for smoke transport and dispersion models.

Chapter 8: A review of modeling approaches used to simulate smoke transport and dispersion

Derek V. Mallia[1] and Adam K. Kochanski[2]

[1]*Department of Atmospheric Sciences, University of Utah, Salt Lake City, UT*

[2]*Department of Meteorology and Climate Science, San José State University, San Jose, CA*

*Corresponding author email: Derek.Mallia@utah.edu

Version: January 28th, 2022; edits from NHF French, ed. on Jan 2nd, 2022.

Book: Fire, Smoke and Health: tracking the modeling chain from flames to health and wellbeing

Running header: Modeling smoke transport and dispersion

Abstract:

A variety of smoke model frameworks are used to simulate smoke for research and forecast applications. Here, a comprehensive summary is provided which covers the many different smoke models that are available, while simultaneously highlighting some of the strengths and weaknesses of each model, along with the uncertainties surrounding each of these frameworks. This review also provides an in-depth discussion on coupled wildfire-atmosphere models, which is a relatively newer smoke modeling tool not previously discussed in other review papers. Key processes related to smoke transport and dispersion, such as the wildfire plume rise, are also discussed in length. This review wraps up with a discussion of future smoke modeling needs and potential new research directions for smoke transport and dispersion models.

1. Introduction

Smoke is a product of the combustion process that contains various chemical species and particulates, which can degrade air quality across a broad range of spatiotemporal scales (Goodrick et al., 2012). Increased fire activity due to climate change (Westerling et al., 2006; Spracklen et al., 2009) and robust population growth across the western U.S. is expected to expose 82 million Americans to smoke in the coming decades (Liu et al., 2016a). As wildfires increase in frequency and intensity, it is imperative that tools are developed and improved upon for studying and forecasting smoke and combustion products detrimental to health, including particulate matter with a diameter less than 2.5 μm ($PM_{2.5}$) and precursors for ozone (O_3) formation downwind of the fire (Jaffe and Widger, 2012). Some objectives of smoke modeling includes limiting the public's exposure to unhealthy concentrations of smoke and determining how smoke could impact active fire management operations during active wildfires and prescribed burns (Kochanski et al., 2018; Peterson et al., 2020). Prescribed burns, for example, are used to manage forests, combat wildfires, and mitigate public exposure to smoke (Rappold et al., 2014). Igniting fires in a controlled setting, limits the intensity and fuel consumption of wildfires, and therefore reduces smoke production relative to uncontrolled wildfires with no fuel thinning (Haikerwal et al., 2015). Smoke models can also be used to forecast meteorology that can favorably disperse smoke from prescribed burns, and to inform burn decisions so that the public's exposure to unhealthy concentrations of smoke is limited (Lahm, 2015). Finally, smoke models are also needed to elucidate processes that govern the chemical makeup and transport of smoke. Such processes range from small-scale mechanisms that drive the wildfire plume rise (Mallia et al., 2020a) to the global impacts of smoke aerosols on climate (Peterson et al., 2018; Christian et al., 2019).

Forecasting and simulating smoke transport is an inherently difficult task as wildfires and smoke transport is a multi-scale phenomenon with many interconnected processes (Figure 1). For example, the wildfire plume rise, which is responsible for injecting smoke in the atmosphere, is controlled by many factors such as atmospheric stability, wind shear, heat fluxes, and fire geometry (Figure 1) (Freitas et al., 2007; 2010). Pyroconvective plumes can also affect local meteorology by increasing near surface winds (Clements et al., 2007; Kochanski et al., 2013), shading areas underneath the plume (Figure 1) from direct insolation (Robock, 1988; 1991; Lareau et al., 2015; Walters et al., 2016; Kochanski et al., 2019), and in rarer cases; plumes can initiate fire-generated thunderstorms (i.e pyrocumulonimbus; Fromm et al., 2010). These processes can often feedback to the local meteorology at the fire line and impact wildfire behavior.

The amount of smoke and heat that is being emitted by the fire serve as essential inputs for smoke models (see #1 in Figure 1). Smoke emissions are used to determine the mass flux of chemical species into the atmosphere while the heat flux and fire area are important variables for determining how far up smoke might be lofted into the atmosphere. However, accurately quantifying fire emissions and heat fluxes from wildfires remains challenging. Estimating smoke emissions and heat fluxes requires information on the exact location and geospatial context of active burning, a description of fuels that are being consumed by the fire, and how intensively that fuel burns (see Chapter 5). Previous work has estimated that uncertainties associated with $PM_{2.5}$ emissions from fires could be as high as 64% (Urbanski et al. 2011). Errors in emission estimates often stem from the errors in the estimated burned area, which can be difficult to quantify due to ambiguities associated with differentiating the burned from unburned areas within and around the fire perimeter (Battye and Battye, 2002). Emission factors for different

chemical species and aerosols emitted by the fire are yet another major source of uncertainty and can exhibit significant variability due to heterogeneous fuel type and condition (Urbanski, 2014), as well as combustion characteristics (flaming vs. smoldering) (Lobert, 1991; Yokelson et al., 1996; Chen et al., 2007; McKeeking et al., 2009; Burling et al., 2010). Lastly, burn severity, which is related to fuel consumption, can also affect emission estimates, and add uncertainties to smoke emission inventories (Urbanski et al., 2011).

Forecasting smoke emissions and heat fluxes adds additional challenges, as it requires a model to make future projections for fuel consumption, on top of the underlying assumptions needed to convert burned biomass into emissions of different chemical species and aerosol particles (see Chapter 7). The uncertainties surrounding fire-emitted fluxes can also influence the vertical plume extent and plume dynamics (Freitas et al., 2007), which in turn, can impact how smoke is transported and dispersed from the fire.

Many atmospheric and chemical modeling frameworks can be used to simulate the transport of smoke from wildfires and prescribed burns. These smoke modeling frameworks range from simple box and Gaussian plume models (Lavdas, 1996) to more sophisticated modeling systems that can simulate smoke on an atmospheric grid with full physics and photochemistry (Hu et al., 2008; Liu et. al, 2009; Hodzic et al., 2007; Grell et al., 2011, Larkin et al., 2009; Kochanski et al., 2016). The primary difference between smoke models is how they account for physical processes that govern smoke transport and dispersion (Figure 1), along with other underlying processes such as fire emissions and burn area, fire-atmosphere interactions, plume entrainment, atmospheric chemistry, aerosol physics and particle deposition, and plume entrainment (Figure 1; Table 1). These models can also differ in terms of the reference frame that they use to simulation smoke, i.e., the Eularian versus the Lagrangian perspective.

The type of model used to simulate smoke often depends on the application and the scientific question or application that the researcher or fire manager is addressing. For example, for some applications, a Gaussian plume models could be more practical for a case where the wind field is unidirectional and constant between the smoke source and receptor. However, if the user attempts to model a case where there is a large wildfire in complex terrain, with erratic wind fields generating intense pyro-convection, a Gaussian plume model may not be sufficient; thus, necessitating the need for a more complex and computationally demanding modeling framework such as a coupled fire-atmosphere model.

In the following sections of this Chapter (Section 2 & 3), we will provide a brief overview of important smoke-related processes (Section 2) while highlighting the different modeling frameworks used to simulate smoke transport (Section 3). Section 3 will be divided by smoke transport model type. This section will then be followed up with a list of plume-rise models, which are often integrated within various smoke transport models to vertically distribute smoke emissions (Section 4). Finally, Section 5 will summarize some of the major discussion points of Sections 2, 3 and 4, while Section 6 will discuss future smoke modeling needs and directions.

2. Smoke-related processes

As discussed in the previous section, smoke models need to represent many critical fire and atmospheric processes such as (1) fire growth or burned area, (2) smoke emissions, (3) the buoyant rise plume rise driven by the fire, (4) mixing between smoke plume and the ambient air outside of it, often referred to as entrainment, (5) deposition processes, (6) downwind smoke dispersion, and (7) plume chemistry (Figure 1). It should be emphasized that these processes do not operate independently, and are sometimes dynamically linked together (Fromm et al., 2010;

Lareau and Clements, 2016; 2017; Kochanski et al., 2019; Mallia et al., 2020a). For example, heat fluxes generated by the fire can sometimes result in intense pyroconvection. If the smoke plume reaches a high enough altitude, water vapor will condense into liquid cloud water that can aid in in the formation of pyrocumulus (pyroCu) or pyrocumulonimbus (pyroCb) clouds. There have been several documented cases of pyroCbs reaching altitudes of 15-km or more (Fromm et al., 2010; Peterson et al., 2018). The range of scales involved in the dynamics of fire-generated plumes is immense as it encompasses small scale processes driving combustion and heat release at a fire front, up through large-scale global weather patterns, which are responsible for driving long-range smoke transport. The processes discussed above are conceptualized in Figure 1.

Currently, most smoke modeling frameworks are developed to deal with smoke transport targeted at specific spatiotemporal scales. It should be emphasized that assumptions made within one model may not necessarily be valid for another model that deals with smoke transport at a different scale. Thus, there is no single model that encompasses the full range of scales needed to explicitly resolve smoke generation, plume rise and dispersion. This concept is conceptualized in Table 1, where individual smoke models have 'niches' in the continuum of spatial and temporal scales. Combustion resolving models such as Wildland-Urban Interface Fire Dynamics Simulator (WFDS; Mell et al., 2007) and FIRETEC (Linn and Cunningham, 2005) operate at smaller scales while, models such as Daysmoke (Achtemeier et al. 2011) or WRF-SFIRE/WRF-FIRE (Mandel et al. 2011; Coen et al. 2013) and others focus on simulating smoke at larger spatiotemporal scales, but at the expense of small-scale processes that need to be simplified as parameterizations. Chemical transport models such as GEOS-CHEM resolves the coarsest processes, but simulates smoke at the largest scale possible (global). Aside from spatiotemporal scales, smoke models can also be classified based on how they represent critical smoke-related

processes and the frame of reference used to simulate smoke.

2.1 Fire burn area and emissions

The fire burned area and emissions, which are related to fire activity, are critical inputs for most smoke models (see Chapters 3 and 5). Fire burned area emission can be represented in several different ways within smoke models. In many cases, models simply rely on external fire emission inventories such as GFED (Van der Werf et al., 2010), FINN (Weidenmeyer et al., 2009), or MFLEI (Urbanski, 2017) to provide historical estimates of smoke emissions and fire area. Some fire emission inventories, such as Missoula Fire Laboratory Emission Inventory (MFFEI), include emission uncertainty estimates using a Monte Carlo analysis (Urbanski et al., 2011). A more comprehensive list and description of fire emission inventories can be found in **Chapter 4**. Satellites are also playing increasing large role to estimate fire emissions and heat fluxes. Operational smoke forecast models, such as HRRR-Smoke (Amohdav et al., 2017), use satellite fire radiative power (FRP) to estimate smoke emissions and heat fluxes, and then scale fire activity by an average fire diurnal cycle. A subset of smoke models, mainly, coupled fire-atmosphere models, can project future fire activity based on a fire spread parametrization that accounts for local meteorology, fuel types and characteristics, and terrain.

FIRETEC and WFDS employ a physics-based approach for estimating fire growth and the burned area. The physics-based approach utilizes models that explicitly represents combustion, heat transfer, aerodynamic drag, and turbulence. These models can predict fire growth, which can be used to estimate the burned area at any time, along with the amount of fuel consumed, and subsequently, smoke emissions. While physics-based models represent the most realistic way to simulate combustion processes and fire progression (where and when a fire moves), they

simplify smoke transport processes such that smoke is assumed to be a passive tracer; thus, ignore smoke chemical transformations and radiative impacts. Finally, explicitly resolving combustion requires very detailed information about fuels at high spatial resolutions (order of meters) and therefore are very computationally demanding. Ultimately, this limits the size of simulated fires to less than 100 acres for physics-based approaches (Liu et al., 2019).

An alternative method for estimating fire progression can be accomplished through empirical-based parameterizations. The most widely used fire progression parameterization is the Rothermel surface fire spread model (Rothermel, 1972), which was developed within the United States Forest Service (USFS) during the 1960 and 1970s. Unlike the physics-based approach, fire spread models, like the Rothermel model, estimate fire growth rates through a quasi-empirical equation that relates fire spread to variables such as fuel type and characteristics, terrain slope, and wind. Since fire spread parameterizations rely on simple algebraic formulas, they estimate fire growth rates at a more modest computational cost (Liu et al., 2019). Coupled fire-atmosphere models such as WRF-SFIRE and WRF-FIRE employ an empirical-based parameterization to estimate fire growth, fuel consumption, fire heat fluxes, and smoke emissions.

2.2 Plume rise

The fire plume rise, *i.e., the vertical transport of smoke*, is yet another important phenomenon that must be accounted for when simulating smoke transport from prescribed burns or wildfires. The plume rise is primarily driven by heat released from the fire along with the atmosphere's response to this heating (Figure 1). Essentially, the fire plume rise acts as a chimney, which can loft smoke high in the atmosphere, with plume rise altitudes sometimes reaching upwards of 15-km in exceptional cases (Fromm et al., 2010; Peterson et al., 2018). The

height over which the plume extends is referred to as the plume injection height and is a function of intensity and geometry of surface fire, ambient atmospheric conditions such as stability, wind shear, and moisture profile, and plume microphysics.

The smoke injection height can control for the fate of smoke, among other factors, such a large-scale weather patterns and convection. For example, when smoke is lofted at a lower altitude, weaker winds near Earth's surface can limit how far the smoke is transported, while particle removal processes such as dry deposition are more dominant near the ground (Zhang et al., 2001; Emerson et al., 2020). For cases of limited smoke transport, smoke can accumulate in areas local relative to the smoke source region, which can further degrade the air quality, locally (Kochanski et al., 2019). Conversely, smoke that is injected higher in the atmosphere will often travel further from the fire and can degrade air quality over a much larger geographical region. At this same time, the fire plume rise can also cause the smoke to overshoot areas near the fire, therefore limiting local impacts of smoke on air quality.

The injection height can also play a vital role on aerosol feedbacks within the climate system. Smoke that is lofted into the upper troposphere and lower stratosphere can have a much longer residence time relative to smoke aerosols injected into the lower troposphere and planetary boundary layer (PBL). Previous research has demonstrated that smoke lofted further up in the atmosphere can have greater impacts on climate forcing (Barnes and Hofmann, 1997; Robock, 2000). The few examples provided above exemplify the need to accurately resolve the fire plume rise for smoke modeling applications.

A variety of different modeling approaches currently exist for quantifying the vertical transport of smoke by fire plume rise (Liu et al., 2010; Paugnam et al., 2016). These models range from simple approximations that release smoke at altitudes that correspond climatological

averages to full-physics models that can explicitly resolve the wildfire plume rise and plume rise dynamics (Trentmann et al., 2006; Kochanski et al., 2016). Sometimes plume rise models are integrated directly within smoke transport models (Larkin et al., 2009; Amohdav et al., 2017) while other frameworks run the plume rise model in an offline setting (Mallia et al., 2018). A separate section in this chapter (**Section 4**) has been dedicated to describing the various plume rise modeling approaches used within smoke transport models.

Work carried out by Mallia et al. (2018) found that simulations of local-scale smoke transport were highly sensitive to the altitude in which emissions were injected at. A regional-based study by Walters et al. (2016) also found that smoke transport within WRF-Chem was sensitive to the plume injection height, with simulated aerosol optical depth values varying by as much as ±50% depending on the plume height injection scheme that was used. In both studies, the simulations that attempted to estimate vertical plume extent performed better than model configurations that injected smoke emissions at single level or at the surface.

While the work outlined above has indicated the plume rise models have improved smoke simulations, several studies have noted inconsistencies between simulated and observed plume top heights (Val Martin et al., 2012; Raffuse et al., 2012). Val Martin et al. (2012) concluded that implementing plume rise models within smoke transport models "remains a difficult proposition" given the uncertainties surrounding the formulations of plume rise parameterizations and model inputs such as fire heat fluxes and area.

2.3 Meteorology

Meteorological models are often needed to simulate the downwind transport of smoke. Numerical weather prediction models (NWP) are the most widely used method for characterizing the three-dimensional structure of meteorological variables such as winds, temperature,

humidity, and pressure. Approximated forms of partial differential equations that describe the atmosphere are used to predict the state of the atmosphere for any given time and location. These equations are solved numerically on an atmospheric mesh that covers the simulated domain (Kalnay, 2003). Certain meteorological processes, such as cloud microphysics, land-atmosphere interactions, and solar radiation are usually too small or too complex to be explicitly accounted for by governing equations. Thus, most NWP models parameterize these processes using a variety of different methods (Kalnay, 2003). Depending on the grid spacing of the meteorological model, certain processes can be either parametrized (if the model resolution is too coarse to resolve them) or explicitly resolved if the model resolution is sufficient (Weisman et al. 2008; Shin et al. 2015). NWP models such as Weather Research and Forecast model (WRF; Powers et al., 2017) operate across a large range of spatiotemporal scales and therefore parameterize processes such as convection in coarser domains but can explicitly resolve convective processes when run at a fine spatial resolution.

In essence, NWP models provide the inputs needed to simulate the transport of smoke from the fire source to the area(s) of interest. Some smoke modeling frameworks, such as WRF-SFIRE (Mandel et al., 2011; Kochanski et al., 2016), WRF-Chem (Grell et al., 2005), and HRRR-Smoke directly account the transport of smoke within the dynamical core of the WRF. Other models, compute the transport of smoke in an offline setting, where output from a NWP model such as WRF, North American Mesoscale Forecast System (NAM) or the Global Forecast System (GFS) is used to trace the transport smoke. Smoke modeling frameworks such as HYSPLIT and CMAQ use the offline method. One benefit of the offline method is that the smoke modeler does not always need to run their own meteorological model, which can be timely and computationally expensive. However, this method does not allow two-way coupling

254 between the smoke and the atmosphere, which can sometimes be important when simulating the
255 interactions between the smoke and meteorology (Kochanski et al., 2019). Smoke models, such
256 as VSMOKE preclude the use of NWP models, and simply assume that the wind fields are
257 steady state, therefore using wind data from a nearby weather station.

258 *2.4 Aerosol physics*

259 Smoke particles directly interact with energy from the sun by scattering and absorbing
260 incoming solar radiation due to the presence of black and organic carbon (Figure 1). Interactions
261 between smoke particles and incoming solar radiation can result in differential heating of the
262 atmosphere that can impact atmospheric stability and/or near-surface temperatures, i.e., aerosol
263 direct effects (Bauer and Menon, 2012). For example, smoke shading effects occurs when
264 incoming energy from the sun is blocked by the opaque smoke plume, which results in cooling at
265 the surface (Robock, 1988; 1991; Trentmann et al., 2006). Smoke shading can impact
266 temperature forecasts, or in more extreme circumstances, it can affect smoke transport (Segal
267 and Arrit,1992; Kochanski et al. 2019). An observational-based field campaign in Northern
268 California found evidence of smoke-induced density currents where differential solar heating
269 between areas with and without smoke resulting in a self-propagating, surfaced-based smoke
270 plume that opposed the ambient wind (Lareau et al., 2015). A modeling-based study carried out
271 by Kochanski et al., (2019) found that localized reductions in incoming solar radiation within
272 smoke-filled mountain valleys reduced surface temperatures while increasing temperatures near
273 the top of smoke layer. In this scenario, there was evidence that smoke was responsible for
274 cooling the surface, suppressing convective boundary layer growth, which effectively limited
275 ventilation between the smoke-filled layer and the atmosphere. In turn, this resulted in an
276 accumulation of smoke and subsequently, more cooling via a nonlinear feedback mechanism.

Smoke particles can also interact with atmosphere via indirect effects where smoke particles alter cloud microphysics (Lindsey at al., 2008; Lee et al., 2018). To summarize, smoke particles can promote the formation of additional cloud water droplets at the expense of larger cloud water droplets since cloud droplets have to compete for a finite amount of water vapor (Andreae et al., 2004). A simulation of a PyroCb in the Texas Panhandle found that the smoke particles played an important role towards enhancing the strength of the convective updraft (Zhang et al., 2019). These results were consistent with Grell et al. (2011) who also concluded that simulated convection over Alaska was stronger in the presence of smoke, albeit the convection produced less precipitation.

Several existing smoke modeling frameworks such as WRF-Chem, WRF-SFIRE, and HRRR-Smoke are equipped to deal with some of the interactions noted above. Other processes not previously discussed, such as wet and dry deposition represent important loss processes for atmospheric particles like smoke (Zhang et al., 2011; Saylor et al., 2019) and are parametrized within most smoke transport models that simulate particulate matter. WRF-Chem contains a full suite of aerosol parameterizations that can account for effects ranging direct aerosol effects to indirect effects that can impact cloud microphysics and PyroCb development (Grell et al., 2011; Zhang et al., 2019). GEOS-Chem is another popular aerosol transport model for simulating smoke transport and for quantifying the impacts of smoke on radiative forcing at the global scale (Christian et al., 2019).

A variety of methods are used within smoke models to simulate aerosol physics. For example, some aerosol schemes use the bulk method where only the total mass of the aerosol compound is known, therefore this is no information about the particle number and aerosol size distribution (Chin et al., 2000). While this method is simple, it is numerically efficient and

computationally cheaper to run. Modal aerosol schemes are slightly more complex in that they include aerosol size distributions using three or more modes that includes the Aitken, accumulation, and coarse modes (Liu et al. 2016b). The most sophisticated method for simulating aerosol physics is through a bin method where aerosols are distributed into many discrete size bins, which are simulated separately (Zaveri et al., 2007). Bin methods are typically computationally expensive to run.

2.5 Chemistry

Smoke plumes are made of a mixture of many chemically active species and aerosols such as nitrogen oxides (NO_x = NO + NO_2), nitrous acid (HONO), volatile organic compounds (VOCs), which can impact air quality through the formation of ozone (O_3), and secondary organic aerosols (SOA) (Andrea and Merlet, 2001; Akagi et al., 2011; Jaffe and Wigder, 2011; Kochanski et al., 2016; Brey and Fischer, 2016; Peng et al., 2020). O_3 is formed through the chemical reaction between molecular oxygen (O_2) and atomic oxygen ($O(^3P)$). The supply of atomic oxygen is driven by chemical reactions involving NO_x and non-methane organic compounds that simultaneously exposed to sunlight photo-dissociate creating $O(^3P)$. Since O_2 is abundant in the atmosphere, O_3 production is typically limited by the availability of NO_x. The most common sources of NO_x are anthropogenic emission sources and wildfires (Finlayson-Pitts and Pitts, 1986).

Smoke plume chemistry is sensitive to several factors including time of day, meteorology, altitude, chemical composition of the plume, combustion efficiency, transport time, and nearby emission sources (Giglio, 2007; Jaffe et al., 2004; Lim et al., 2019; Peng et al., 2020). Smoke shading effects within the plume can also reduce O_3 production by limiting photochemical

reactions (Jaffe and Wigder, 2011) producing molecular oxygen. The sequestration of NO_x as the smoke plume ages can also limit O_3 production downwind of the fire (Tanimoto et al., 2008). Due to the complex and non-linear interactions between O_3 and other chemical processes, accurately simulating O_3 chemistry within smoke can be difficult (Jaffe and Wigder, 2011; Kochanski et al., 2016).

There are several existing modeling frameworks that have been used to both better understand smoke plume chemistry and to make air quality forecasts for chemical species such as O_3. The Community Multiscale Air Quality (CMAQ) model is a state-of-the-art air quality model that can simulate many atmospheric chemical processes related to gas, aqueous, and aerosol phase chemistry (Sarwar et al., 2011; 2013). Therefore, models such as CMAQ can simulate complex chemistry associated with O_3 and SOA. Operational air quality modeling frameworks such as AIRPACT (http://lar.wsu.edu/airpact/) are based on the CMAQ model (**see Chapter 9**). CMAQ generally estimates anthropogenic emissions using the Sparse Matrix Operator Kernal Emissions (SMOKE; https://www.cmascenter.org/smoke/) combined with fire emissions defined by the Satellite Mapping Automated Reanalysis Tool for Fire Incident Reconciliation (SmartFire2)–BlueSky framework (Larkin et al., 2009). WRF-Chem and WRF-SFIRE-Chem have also been used to simulate chemical reactions within wildfire plumes (Pfister et al., 2011; Kochanski et al., 2016). For example, work by Kochanski et al. (2016) integrated WRF-SFIRE with WRF-Chem's Model of Ozone and Related chemical Tracers (MOZART; Emmons et al., 2010) chemical mechanism to forecast O_3 for the 2007 Witch-Guejito Santa Ana fires. Chemical models such as WRF-Chem and CMAQ also need chemical boundary conditions from either a larger-scale chemical transport model or a data assimilation product that utilize satellite observations. This is covered more in-depth in **Chapter 7**.

3. Smoke transport models

3.1 Box model

Box models are one of the simplest approaches used to simulate smoke exposure (Letteau 1970). As suggested by the name, a box model assumes that air for a specified domain can be represented by a box, which is often bounded by the surface and the top of the PBL. Smoke within the box model is often assumed to be instantaneously diluted throughout the entire column, thus eliminating the need to simulate smoke dispersion and the fire plume rise. Because of relative simplicity of the underlying assumptions within a box model, these models are easy to run, and require limited computational resources (Goodrick et al., 2012).

Box models have been previously used for smoke management applications in mountain valleys, where the lateral boundaries of the box are bounded by valley walls. Research presented Brown and Bradshaw (1994) indicated that while box models struggle with predicting near-surface smoke concentrations from local fires, these models can be useful for assessing smoke loading within remote mountain valleys for prolonged smoke episodes. Another study by Pharo et al. (1976) found that box model tended to overestimate smoke concentrations near fires. It was hypothesized that overestimated smoke concentrations stemmed from the instantaneous dilution assumption made by box models, which is not valid in the vicinity of the fire where the plume dynamics and interactions with winds and atmospheric stability control mixing and dilution.

Zero-dimensional box models are also popular choice for simulating complex atmosphere chemistry within smoke plumes for research-based applications (Wolfe et al., 2016; Decker et al., 2021). Zero-dimensional box models are deployed by atmospheric chemists to investigate different chemical mechanisms (Archibald et al., 2010), analyze field observations (Decker et al.,

2021), and for laboratory chamber experiments (Paulot et al., 2009). The models are particularly useful for understanding specific chemical processes, developing conceptual models, and testing hypotheses through sensitivity experiments (Wolfe et al., 2016).

3.2 Gaussian plume model

The Gaussian plume model represents the simplest way for simulating the downwind transport of smoke. Instead of letting smoke dilute within a targeted domain like what is done for box models, the Gaussian plume model attempts to account for atmospheric transport and dispersion (Taylor, 1922). Crosswind transport, i.e., dispersion is parameterized as a Gaussian distribution that takes the form of a steady state solution of the advection-diffusion equation. The direction of the smoke transport is determined by the wind speed and direction. Since winds are assumed to be constant in time and space, smoke is assumed to travel in a straight line from where it is emitted until it reaches the end point of the smoke plume or model domain. As a result, areas that frequently experience highly variable weather phenomena such as sea breezes, frontal passages, and mountain-valley circulations may not be appropriate for a Gaussian plume model. However, for cases where meteorological conditions are homogenous, Gaussian plume model models can be an ideal tool for simulating downwind horizontal smoke transport given the limited computational demands and model inputs for these models.

As of today, there are two smoke models that utilize Gaussian plume theory to simulate smoke transport and exposure. VSMOKE (Lavdas, 1996) is often used by land managers in the Southeastern U.S. to provide a quick and simple estimate of smoke impacts for prescribed burns based on planned fire activity and weather forecasts (Jackson et al., 2007). No wildfire plume rise is used within VSMOKE, thus the user must specify a fraction of smoke that is released near

the ground and at the PBL. For smaller prescribe burns, its generally safe to partition most of the smoke emissions within the PBL. However, for larger prescribe burns and wildfires, this assumption could be inadequate, as the fire plume rise can sometimes inject smoke into the free troposphere (Banta et al., 1992). The Simple Approach Smoke Estimation model (SASEM; Sestak and Fiebau, 1988) is another Gaussian plume model that was designed to estimate smoke transport across relatively flat terrain. Like VSMOKE, SASEM can estimate ground-level smoke concentrations. SASEM can also estimate visibility impairment and the height of the fire plume rise as predicted by the Briggs (1975) plume rise model (see **Section 4b**). SASEM is mostly used for prescribed burns in the state of Arizona (Goodrick et al., 2012).

3.3 Puff models

Puff models represents another class of dispersion models, which reduces the number of assumptions made by Gaussian plume models (Lin, 2012). The Puff model represents the smoke plume as a collection of independent smoke "puffs" that are assigned an average smoke concentration that is representative of the puff's volume. Puffs are constantly released throughout the duration of a burn, with each puff having a total mass of smoke that is related to the smoke emissions at the time of when the puff was emitted from the fire (Goodrick et al., 2012). Once the puffs are released into the atmosphere, they are transported by winds that can vary in time and space, unlike Gaussian plume models. Since Puff models follows a fluid parcel as it travels through time and space, e.g., moving reference frame, these models are classified as being Lagrangian.

Puff models are well suited for areas with lots of variability in winds such as mountainous areas and coastlines. The effects of diffusion and entrainment are also accounted by Puff models.

For cases where the Puff's volume increases, the smoke concentration within the Puff would decrease, while a decrease in the Puff's volume would correspond in an increase in smoke concentration. While Puff models represent a significant step forward relative to Gaussian plume modeling approaches, areas with strong wind shear and turbulence can distort puffs into non-Gaussian shapes (Lin, 2012). In these situations, ad hoc parameterizations such as puff splitting or merging are often necessary (Walcek, 2002).

CALPUFF (Scire et al. 2000) and Hybrid Single-Particle Lagrangian Integrated Trajectory (HYSPLIT; Draxler and Hess, 1997) are the most commonly used model frameworks that utilize Puff models. The CALPUFF model is driven by a diagnostic meteorological model (CALMET) that grids variables such as winds, temperature, PBL heights, friction velocity, and the Monin Obukhov length on a three-dimensional micrometeorological domain. The three-dimensional data is either obtained by interpolating meteorological data from nearby near-surface and upper-air observations and/or from a Eulerian NWP model. CALPUFF is commonly used by the Environmental Protection Agency to assess the impact of atmospheric pollutants on air quality for an area of interest (Scire et al., 2000). Even though CALPUFF does not explicitly resolve the plume rise, it utilizes the Brigg plume rise parameterization to estimate the injection height of atmospheric pollutants. Several studies have used CALPUFF for assessing the impacts of fires on different airsheds across North America. In one study, CALPUFF was used to quantify the impacts of agriculture burning for areas along the USA-Mexico border (Choi and Fernando, 2007). Converting fire activity, fuel conditions, and burn time into smoke emissions was listed as one of the major limitations of simulating smoke with CALPUFF. Jain et al. (2007) found that smoke plumes from agriculture burns in the Pacific Northwest exhibit large variability and were sensitive to fire input parameters when using CALPUFF. Despite the uncertainties associated

with meteorology and fire input parameters, CALFPUFF was mostly able to reproduce surface $PM_{2.5}$ concentrations when evaluated with nearby air quality stations.

HYSPLIT is another modeling framework that can be used to simulate the transport of pollutants as puffs, single trajectories, or an ensemble air parcel trajectories, with the latter being discussed more in **Section 3d**. Similar to CALPUFF, an external three-dimensional NWP model needs to provide meteorological inputs such as temperature and wind to determine transport pathways for puffs within HYSPLIT. A joint project between the United States National Oceanic and Atmospheric Administration (NOAA) and the Australia's Bureau of Meteorology led to the implementation of several modules, which allow HYSPLIT to account for chemical reactions in the atmosphere. HYSPLIT's puff model assumes that puffs continuously grow until they reach a size threshold that is larger than the meteorological grid cell. Once puffs reach the size threshold, they are split up into smaller puffs with identical properties in terms of pollutant concentrations.

3.4 Lagrangian Particle Dispersion models

While Puff models can account for changing flow fields, these models make many assumptions regarding the expansion and contraction of the puff, along with interactions between different puffs. Lagrangian particle dispersion models (LPDMs) attempt to rectify some of these issues by simulating atmospheric transport as an ensemble of particles, with each particle representing a parcel of air with equal mass. These particles possess several important properties such as (1) being small enough where they can follow the wind field without becoming deformed, but (2) much larger than the average distance between air molecules, and (3) have fluid properties that are nearly identical to the surrounding air; thus, are unaffected by gravitational settling and/or buoyancy (Lin, 2012). These particles are transported by the mean

wind ($\bar{\mathbf{u}}$) and a stochastic turbulent component ($\mathbf{u}'$), which can be parameterized as a Markov process (Lin, 2012). As a result, these models are well-equipped to handle cases with strong turbulence and/or wind shear. Simulated particles can also be referred to as trajectories. Since LPDM models must use thousands of particles to accurately depict turbulent dispersion (Mallia et al., 2015), these models are more computationally expensive than puff models. However, the downside of the added computational cost of simulating thousands of particles through three-dimensional space is generally outweighed by LPDM's ability to naturally simulate the effects of turbulence and wind shear. Several LPDM models are currently used to simulate smoke from prescribed burns to reduce human exposure to smoke or used for research-based applications. For example, LPDMs have been deployed in inverse-based studies to better understand spatiotemporal variability of fire emissions (Kim et al., 2020). LPDM models have also been used to identify major source regions of wildfire smoke and to quantify the role of the wildfire plume rise on smoke transport (Mallia et al., 2015; 2018).

FLEXPART (Stohl and Thomson, 1999) is a LPDM model that simulates long-range atmospheric transport and dispersion for a many atmospheric pollutants, tracers, and greenhouse gases. FLEXPART parameterizes the effects of wet and dry deposition. FLEXPART was first applied to wildfire smoke by Wotawa and Trainer (2000), who used FLEXPART to examine the impacts of Canadian wildfires on air quality in the southeastern U.S. Based on simulated results from FLEXPART, Wotawa and Trainer (2000) found that wildfire smoke was large responsible for elevated concentrations of carbon monoxide (CO) during the summer of 1995. FLEXPART was integrated with the National Observatory of Athens FireHub platform (http://ocean.space.noa.gr/fires) to simulate smoke plumes over Greece. An analysis carried out Solomos et al. (2015) found that FLEXPART, driven by winds from WRF, was able to capture

long-range smoke transport over Greece, along with transport near complex terrain features such as mountains and coastlines. A column-based plume rise model was integrated within FLEXPART to handle the vertical transport of smoke due to the fire plume rise.

DaySmoke (Achtemeir et al., 2011) is another model that uses Lagrangian-based framework to simulate downwind smoke transport. DaySmoke was originally built off the ASHFALL model, which was used to simulate deposition of ash particles from agriculture fires. Today, DaySmoke is used to simulate smoke dispersion to limit smoke exposure of communities downwind of prescribed burns. DaySmoke consists of 4 components for simulating smoke, including an entraining torrent model, a detraining particle model, a large eddy parameterization used to simulate the PBL, and a smoke emissions model, which describes the emission history prescribed burns. The entraining torrent model handles the effects of convective uplift from the fire plume rise. In addition, the convective updraft within DaySmoke can be separated into multi-core updrafts, which have weaker updrafts, smaller diameters, and are more sensitive to the entrainment. Ultimately, the separation of the convective updraft into multiple cores can limit the altitude at which smoke is injected, thus correctly specifying the number of updraft cores is critical when simulating the fire plume rise (Liu et al., 2010). Once the smoke particles are discharged from the smoke plume, they are traced through the atmosphere by a mean and turbulent wind component (Achtemeir et al., 2011). Like other LPDM models, the turbulent or convective mixing component is considered stochastic. Since DaySmoke employs relatively simple physics and no chemistry, the model requires less computational resources relative to other smoke modeling frameworks.

HYSPLIT is a popular tool for simulating smoke transport at larger scales (10-1000 km), and can be run as a LPDM or, as previously mentioned as a puff model, depending on the options

selected at runtime (Draxler and Hess, 1997). HYSPLIT has been integrated with the BlueSky modeling framework (Larkin et al., 2009; O'Neill et al., 2008), which utilizes fuel maps and fire consumption rates to estimate smoke emissions (https://www.arl.noaa.gov/hysplit/smoke-prescribed-burns/). The meteorology used to drive HYSPLIT trajectories generally comes from an external NWP model such as the many model outputs provided by the National Centers for Environmental Prediction (NCEP).

The Stochastic Time-Inverted Lagrangian Transport (STILT) model (Lin et al. 2003), which is based off HYSPLIT and has since been merged back with HYSPLIT (Loughner et al., 2021) is another LPDM that has been used to simulate the impacts of smoke on air quality across the Western U.S. (Mallia et al., 2015). Smoke emissions used by STILT can be vertically distributed using the Freitas plume rise model (Freitas et al., 2007; Mallia et al., 2018). STILT typically uses 'backward' trajectories to determine the origin of air that is arriving at a receptor location. Backward trajectories can be used to derive the footprint for a receptor which can then be mapped with smoke emissions to determine contributions of smoke from upwind fires (Figure 2a). The receptor-orientated approach used by STILT makes this modeling framework particularly useful for identifying fires responsible for deteriorating air quality as seen in Figure 2b. Since the NWP models used to drive backward trajectories are often imperfect, STILT has the unique ability to translate wind errors into modeled smoke uncertainties (Figure 2b) (Mallia et al., 2015).

3.5 Eulerian grid models

Smoke transport can also be simulated from the Eulerian perspective where instead of following a puff or particle in a moving coordinate system, a Eulerian 'grid model' simulates smoke transport on a fixed reference plane. A Eularian model can be visualized as collection of

individual cubes that are stacked within a large box, with the box being representative of the lateral boundaries of the model. Equations used to describe the transport of smoke are then solved for each individual cube, which is often referred to as a model grid cell. While tracking individual smoke plumes with a Eularian based model can be more difficult, grid models are more suited for simulating interactions between different plumes and for determining how anthropogenic emission sources might interact with these plumes to form secondary pollutants like O_3 (Goodrick et al., 2012). Eularian grid models heavily rely on NWP models to determine how smoke is transported throughout the model domain. Meteorological data can be provided as an input for Eularian-based smoke models or smoke transport and chemistry can be solved inline with the meteorology. One potential limitation of Eulerian-based frameworks is that emissions are assumed to be instantaneously diluted through model grid cells, which can be unrealistic, especially in coarser-scale model simulations (Goodrick et al., 2012).

CMAQ is a state-of-the-art air quality model, which is one of the most widely used tools for air quality applications. Such applications include regulatory and policy analysis, research, and operational forecasting (Byun and Schere, 2006; Baker et al., 2018). CMAQ contains a suite of atmospheric chemistry and emission routines that enables the model to simulate smoke-related chemical and aerosol processes such as photochemistry, SOA formation, and advanced aerosol physics. While CMAQ does not simulate its own meteorology, NWP model data can be provided as an input, or the model can be coupled directly with the WRF model (Zou et al., 2019). Routines exist within CMAQ, where smoke can be injected between two specified vertical levels either by the user or by an offline plume rise model. AIRPACT (http://lar.wsu.edu/airpact/), which is an operational model used to make air quality forecasts across the Pacific Northwest, is an example of an air quality modeling system that uses CMAQ driven by an external WRF

553 model and fire emissions generated from BlueSky. More details on AIRPACT can be found in
554 the **Chapter 9**.
555 Another popular choice for simulating smoke is with WRF-Chem, which is a chemical
556 transport modeling framework that can simultaneously model meteorology, aerosol physics, and
557 chemical transformations in the atmosphere (Grell et al., 2005). Since the chemical and aerosol
558 modules within WRF-Chem are directly coupled with the dynamical core and physical
559 parameterizations, smoke emissions can modify weather conditions through smoke shading
560 and/or cloud microphysical processes. This type of coupling is unique to modeling frameworks
561 like WRF-Chem, where smoke simulations are computed in-line with meteorology.
562 Smoke emissions within WRF-Chem are typically provided by an external emission
563 inventory such as Fire Inventory from NCAR (FINN; Weidenmeyer et al., 2010), while smoke
564 can be vertically distributed within WRF-Chem using the Freitas et al. (2007) plume rise model.
565 A study by Grell et al. (2011) found that smoke emissions had the potential to affect mesoscale
566 (10-100 km) weather patterns across Alaska by changing vertical temperature and moisture
567 profiles in areas absent of cloud cover. Sensitivity tests also revealed that high concentrations of
568 $PM_{2.5}$ were responsible for altering cloud microphysical processes, which ultimately impacted
569 the modeled spatiotemporal distribution of precipitation across Alaska in 2004. The National
570 Oceanic and Atmospheric Administration (NOAA)'s operational smoke forecast system, HRRR-
571 smoke is based on WRF-Chem v3.9, with several in-house modifications related to smoke
572 aerosol physics (Amohdav et al., 2017). More details on HRRR-smoke can be found in **Chapter**
573 **9**.
574 Global-scale simulations of smoke transport can be achieved with modeling frameworks such
575 as GEOS-Chem (http://acmg.seas.harvard.edu/geos/), which has been used in previous work to

isolate the impacts of wildfire smoke on global climate and air quality (Christian et al., 2019; Li et al., 2020). Like CMAQ and WRF-Chem, GEOS-Chem includes chemical and aerosol routines to simulate changes in the chemical composition of the atmosphere (Bey et al., 2001). Meteorology for GEOS-Chem is provided as an input from an external global NWP model, while smoke emissions are estimated using GFED or FINN. Since GEOS-Chem is a global model, the horizontal grid spacing within the model is very coarse relative to the grid spacing of the other models presented in this chapter. Despite having a coarser model resolution, GEOS-Chem is one of the few models specifically designed to simulate the large-scale impacts of smoke on global air quality, weather, and climate.

3.6 Coupled fire-atmosphere models

Advancements in computational facilities have led to the development and deployment of coupled fire-atmosphere models. Like Eulerian grid models, these coupled fire-atmosphere models simulate smoke transport on a three-dimensional grid. Coupled-fire atmosphere models also simulate their own meteorology using a computational fluid dynamics weather prediction model. Unlike some of the Eulerian grid models discussed in the previous section, coupled fire-atmosphere models simulate fire progression using a formula that parameterize fire growth based on local meteorology, terrain, and fuel characteristics (Mandel et al., 2011), or through the explicit representation of combustion processes (Mell et al., 2007; Mell et al., 2010; Linn et al., 2002; Linn and Cunningham, 2005).

Coupled fire-atmosphere models can utilize information about the predicted burned area and fuel loading to forecast fuel consumption, heat fluxes, and smoke emissions. The heat fluxes forecasted by these models can also dynamically interact with the atmosphere, which allows

coupled-fire atmosphere models to explicitly simulate phenomena such as the wildfire plume rise (see **Section 4d**) and fire-induced winds near the fire front. Some coupled fire-atmosphere models such as WRF-SFIRE can simulate the impacts of smoke on meteorology through aerosol physics and chemistry coupling (Kochanski et al. 2016; Kochanski et al. 2019). While coupled fire-atmosphere models represent the most sophisticated way to simulate smoke, these models can be computationally demanding compared to other models due to the computations needed to resolve near-fire circulations and plume dynamics. However, multi-scale coupled fire-atmosphere models such as WRF-FIRE and WRF-SFIRE use a nested domain setup that allows these models to embed small-scale, high-resolution domains within larger and coarser computational domains. Ultimately, this allows modeling frameworks like WRF-FIRE and WRF-SFIRE to simulate smoke dispersion across large distances at a relatively lower computational cost. Outside of forecasting applications, coupled fire-atmosphere models are ideal tools for studying how fire and fire behavior dynamically interacts with the atmosphere.

FIRETEC and WFDS use a finite-volume, large eddy simulation to model fine-scale meteorological flows near the fire of interest. Here, large eddies within turbulent flow are explicitly resolved by within the numerical grids of FIRETEC and WFDS, while smaller eddies are parameterized with sub-grid scale models (Mell et al., 2007; Linn and Cunningham, 2005). Typically, the grids used by FIRETEC and WFDS are on the order of meters. Since FIRETEC and WFDS use a physics-based approach for simulating fire growth and combustion, detailed information about fuels and fuel density on a scale ~1-m is needed. This attention to detail comes at a cost as FIRETEC and WFDS simulations are computationally expensive to run. Therefore, these models are only feasible for research-based applications. Furthermore, the model grid spacing used within FIRETEC and WFDS also limits these models to individual fire-scale

problems that are typically less than 100 acres in size. Due to the domain size limitations associated with FIRETEC and WFDS, these models are better suited for describing fire behavior and hyper-local smoke transport (Liu et al. 2019). While models such as FIRETEC and WFDS can represent detailed combustion processes and the fire-atmosphere interactions, they do not account for the microphysical and radiative impacts of smoke on the atmosphere or chemical transformations of smoke downwind from the fire.

Models such as WRF-FIRE and WRF-SFIRE operate on a slightly different scale than FIRETEC and WFDS, so that they can be used in both research and forecast applications. To reduce computational costs, fire growth within WRF-FIRE and WRF-SFIRE is parameterized using an empirical formula instead of taking a physics-based approach (Mandel et al., 2011; Liu et al., 2019). While models such as WRF-FIRE and WRF-SFIRE parameterize fire growth rates, heat fluxes generated from the modeled fire are dynamically coupled to the atmosphere. Typically, these models resolve fire progression on scales on the order of tens of meters, while the meteorology from WRF, which is used to drive the fire and simulate smoke transport, is solved on grid with a horizontal grid spacing between 400-1,300m (Kochanski et al., 2019). This allows models such as WRF-FIRE and WRF-SFIRE to simulate smoke across a larger domain compared to FIRETEC and WFDS. In addition, WRF-based modeling frameworks use a nested domain configuration where meteorology and smoke simulated in the innermost domain centered on the fire is fed into subsequently coarser, but larger domains. Despite using a coarser atmospheric grid relative to FIRETEC and WFDS, both WRF-FIRE and WRF-SFIRE can explicitly resolve the wildfire plume rise and first order fire-atmosphere interactions (Liu et al., 2019). Both models treat smoke as a passive tracer, with smoke emissions being estimated based on the fuel consumed by the simulated fire.

WRF-SFIRE was recently coupled to WRF-Chem to allow smoke generated by the fire to undergo chemical transformations while smoke aerosols can be scavenged from the atmosphere. Coupling with the WRF-Chem's aerosol model (GOCART) also allows smoke to interact with atmospheric radiation, therefore allowing WRF-SFIRE to account for smoke shading effects. This type of coupling is unique to only WRF-SFIRE. Preliminary work carried out by Kochanski et al. (2016) found that WRF-SFIRE, coupled with WRF-CHEM was able to reproduce elevated concentrations of NO_x and $PM_{2.5}$ for two large fires in Southern California during the 2007 fire season. A follow up study by Kochanski et al. (2019) found that WRF-SFIRE simulations were able to capture smoke shading effects within mountain valleys across northern California. A positive feedback mechanism was also identified where smoke aerosols resulted in cooler temperature at the surface, which allowed additional smoke aerosols to accumulate at the base of mountain valleys. WRF-SFIRE simulations coupled with WRF-Chem were also used to forecast a wildfire smoke event in Salt Lake City, UT during the summer of 2018. WRF-SFIRE smoke simulations during this event were able to skillfully capture the orientation and shape of the plume, along with local-scale nocturnal mountain valley circulations (Figure 3) (Mallia et al., 2019).

4. Plume-rise models

4.1 Simplified approaches

Earlier smoke modeling frameworks often assumed that smoke from biomass burning was either injected at a fixed altitude, evenly distributed throughout the PBL (Pfister et al., 2008; Hyer and Chew, 2010), assumes some type of ratio for partitioning emissions between the PBL and free troposphere (FT) (Turquety et al., 2007; Leung et al., 2007; Elguindi et al., 2010), or is

prescribed based on local measurements such as satellite (Chen et al., 2009). For continental-scale smoke simulations across North America, the vertical distribution of smoke was found to be insensitive to the modeled plume injection height. It was hypothesized by Chen et al. (2009) that strong summertime convection tends to mix smoke throughout the troposphere, which limited the influence of the plume injection height on vertical smoke distributions.

4.2 Empirical

Another way to estimate the plume injection height is through empirically based models, which require inputs such as buoyancy, fire power, fire area, and/or generalized characteristics of the atmosphere such as atmospheric stability or the PBL height.

The Briggs equations (Briggs, 1975), which is one of the first plume injection models, was originally developed to estimate the height of plumes released from smokestacks. Today, the Briggs equations are commonly used by smoke modeling frameworks such as CMAQ, BlueSky and HYSPLIT. The Briggs model consists of a series of equations used for different stability conditions and whether the plume is momentum or buoyancy dominated. The plume injection height estimated by the Briggs model is a function of buoyancy, ambient wind speeds, and stability. Since the Briggs formulas contain no direct input for the fire heat release, the fire heat release needs to be converted into a buoyancy flux (Raffuse et al., 2012). Plume rise results with the Briggs model have been mixed, which is reasonable considering that it was originally developed to model plumes from smokestacks. Work by Raffuse et al. (2012) and Gordon et al. (2018) found that the Briggs model typically underestimated plume rises, especially for larger wildfires. Achtemeier et al. (2011) hypothesized that models like Briggs are unable to account for microphysical impacts such as latent heat releases. As a result, the Briggs model is unable to account for extreme pyroconvection like pyrocumulus or pyrocumunimbus clouds. However,

691 Achtemeier et al. (2011) suggests that the Briggs model may perform better for smaller wildfires
692 and prescribed burns.

693 A newer methodology for estimating wildfire smoke plume heights was presented in (Sofiev
694 et al., 2012). Like the Briggs models (Briggs, 1975), this methodology uses a semi-empirical
695 formula to estimate fire plume tops. This parameterization uses an energy-balance-based
696 approach to estimate plume tops, similar to convective cloud parameterizations used within
697 larger-scale atmospheric models. The plume height within the Sofiev et al. (2012) scheme is
698 estimated from the following:

699 $$H_p = \alpha zi + \beta\left(\frac{FRP}{P_{f0}}\right)^{\gamma} exp\left(\frac{-\delta N_{FT}^2}{N_0^2}\right)$$

700 where α is part of the PBL passed freely, β weights the contribution of fire intensity, γ
701 determines the power-law dependence on the fire radiative power (FRP), δ weights the
702 dependence of the stability of the FT on the plume rise height (H_p), P_{f0} is the reference fire
703 power (P_{fo} = 10^6 W), N_0^2 is the Brunt-Vaisala frequency reference number (N_0^2 = 2.5 x 10^{-4} s^{-2}),
704 and N_{FT}^2 is the Brunt-Vaisala frequency of the FT. A learning subset of satellite fire smoke plume
705 observations from the Multi-angle Imaging SpectroRadiometer (MISR) were then used to
706 determine the value of the empirical calibration constants (α, β, γ, δ) where α represents is the
707 part of the plume that passes freely through the PBL, β accounts for the weighted contribution
708 from the fire intensity, γ quantifies the power-law dependence of the fire's FRP on the plume
709 height, and δ defines the plume top dependence on the atmospheric stability within the free
710 troposphere.

711 Results in Sofiev at el. (2012) found that their methodology outperformed both the Briggs
712 and 1-D column models when applied to 2000 fire plumes from an independent MISR database

713 across North America and Siberia. One potential limitation of this model is that the parameters
714 defined in Sofiev at el. (2012) are primarily tuned for shallower smoke plumes, since the training
715 data set to develop the parameters only included plume rises with heights less than 4-km
716 (Paugnam et al., 2016).
717
718 *4.3 Column models*
719 Another way for estimating plume top heights is through one-dimensional column models
720 such as the Freitas et al. (2007; 2010) model. The Freitas plume rise model is based off a plume
721 model develop by Latham (1994), which simulates the wildfire plume rise using the equations
722 for vertical momentum, first law of thermodynamics, mass continuity, and cloud microphysics.
723 In addition, the effects of entrainment near the edges of the plume are also parameterized as two
724 entrainment coefficients, with one accounting for the effects of turbulence plume edge, and the
725 other describing for ambient wind shear effects. The final plume injection height is often used
726 within chemical and smoke transport models such as WRF-CHEM (Grell et al., 2005; Pfister et
727 al., 2011; Sessions et al., 2011), STILT (Mallia et al., 2018), and HRRR-smoke. One added
728 benefit of a column-based approach is that this method can provide the vertical plume
729 characteristics, in addition to the final injection height (Figure 4). The final injection height is
730 typically assumed when the upward vertical velocity w reaches 0 m s^{-1}. Since the Freitas plume
731 rise model is cloud resolving, it can simulate moist pyroconvection. The Freitas model's ability
732 to simulate moist pyroconvection can be seen in Figure 4, which shows a secondary increase in
733 vertical velocity between 2.5 – 5 km that is collocated with an increase in liquid cloud water and
734 latent heat releases.
735 Inputs for the Freitas plume rise model includes a one dimensional profile of ambient

736 atmospheric conditions such as temperature, relative humidity, and wind speed, along with
737 surface boundary conditions provided by the fire, i.e., heat flux and fire area. Natively, the
738 Freitas model assumes fire heat fluxes and area based on the vegetation type that is being burned.
739 The heat flux and fire area are then used to compute a buoyancy flux (F) following the
740 expression derived by Viegas et al. (1998):

741 $$F = \frac{gR}{c_p p_e} r^2$$

742 where g is equal to the gravity constant (g = 9.81 m s^{-1}), R represents the ideal gas constant (R =
743 287 J K^{-1} kg^{-1}, c_p denotes specific heat at a constant pressure (c_p = 1004 J kg^{-1}), p_e is the ambient
744 surface pressure, and r defines the radius of the fire. The buoyancy flux can be used to compute
745 the near-surface vertical wind velocity and temperature.

746 More recent work by Val Martin et al. (2012) tried alternative methods for prescribing fire
747 input parameters, such as using satellite FRP to estimate sensible heat fluxes and aggregating
748 satellite fire pixels to construct burned areas. This method resulted in slightly improved
749 simulated plume rises when compared to satellite observations, however, the authors note the
750 Freitas model was unreliable for identifying plumes that were injected into the FT. It was
751 hypothesized that model errors in plume rises likely stemmed from uncertainties surrounding fire
752 input parameters rather than plume rise model formulation. A study conducted by Mallia et al.
753 (2018) showed the Freitas model was able to realistically capture the plume rise for an
754 extensively instrumented prescribed burn in Eglin Airforce Base, FL, when driven by observed
755 fire heat fluxes and burned area. It should be noted however, that this analysis was carried out for
756 a single case study, for a relatively small burn (area = 1.51 km^2), where no pyroCu or Cb activity
757 was observed.
758

759 *4.4 Fully physical* three-dimensional *representation of plume dynamics*

760 Continued advancements in computational resources have resulted in a newer generation
761 smoke models that can explicitly resolve wildfire plume rises. For the full physics method, heat
762 fluxes from the fire are injected directly into the near-surface grid cells of a high-resolution
763 three-dimensional atmospheric model (Goodrick et al., 2012). Like the column-based approach,
764 the atmosphere will respond to the fire heating by generating a buoyant convective plume. One
765 way that this approach different from the column-based approach is that here the plume is
766 resolved in three-dimensional space instead of one-dimensional. In addition, these models
767 typically run at a fine enough resolution where key processes such as entrainment, multiple
768 plume cores, pyroconvection and upward smoke transport are directly simulated by the model,
769 instead of being parameterized. The full physics approach typically requires the model to have a
770 sufficiently fine grid-spacing so that the model can explicitly resolve plume rise dynamics while
771 simultaneously having the volume needed to encompass the convective plume (Goodrick et al.,
772 2012). As such, short model time steps, combined with fine grid cells, often covering a large
773 volume, can drastically increase computational resources needed to explicitly resolve the wildfire
774 plume rise.

775 Directly simulating the wildfire plume rise using a fully physical approach was first
776 pioneered by Trentmann et al. (2006) and Luderer et al. (2006), who used a high-resolution
777 atmospheric model to simulate extreme pyronvection over the Chisholm wildfire located in
778 Alberta, Canada. The plume rise associated with the Chisholm wildfire reached an altitude of 13-
779 km, according to radar observations. The plume rise simulations carried out by Trentmann et al.
780 (2006) and Luderer et al. (2006) were able to replicate the intense pyroconvection observed
781 during this event while also illustrating how meteorological dynamics are coupled with large

782 wildfires. Coupled fire-atmosphere models such as WRF-SFIRE and WRF-FIRE also explicitly
783 resolve the wildfire plume rise. WRF-SFIRE simulations conducted by Kochanski et al. (2016;
784 2018) and Mallia et al. (2020a) found that modeled plume top heights compared reasonably well
785 to satellite-estimated plume heights (average error = ± 500 m). An example of a full physics
786 simulation of a wildfire plume rise by WRF-SFIRE can be seen in Figure 5.
787
788 **5. Summary**
789 The number of large and devastating fires are expected to increase in the coming decades,
790 which will expose communities to poor air quality. Therefore, smoke models will be an
791 important tool for limiting the public's exposure to degraded air quality through smoke forecasts
792 and for determining the optimal time for igniting prescribed burns. Wildfires are also projected
793 to emit more aerosols into the atmosphere, which can affect weather and climate if the smoke is
794 injected high up into the atmosphere (Peterson et al., 2018).
795 Within this chapter, we've provided a brief introduction to the different types of smoke
796 models that are available for researchers, and air quality and land/fire managers alike. This
797 chapter reviews models that range from simple box and Gaussian plume models to more
798 sophisticated modeling systems that can simulate smoke on an atmospheric grid with full physics
799 and photochemistry. Also provided in this chapter is an in-depth discussion on coupled fire-
800 atmosphere models, which has not been included in other review articles. This chapter also
801 reviews processes that are important in the context of smoke transport and how these
802 fundamental processes are resolved within smoke modeling frameworks.
803 While we attempt to cover all smoke models that are available to researchers and managers,
804 covering every smoke model in existence would prove to be an exhaustive effort that could

probably be a book in itself! Nonetheless, we attempt to present a description of a diverse range of smoke transport and dispersion models to the reader. Ultimately, there is no smoke modeling tool that can be treated as a "silver bullet" as each of the models presented here have strengths and weaknesses that are dependent on the application that the model is being used for. Thus, we emphasize that determining the best smoke model for any given application will be dependent on the needs of the user and *what they need* the smoke model to do.

6. Future directions

Fundamentally, the processes that govern smoke transport and dispersion are well understood, especially in the absence of significant pyroconvection (Goodrick et al., 2012). However, processes related to the fire plume rise (Val Martin et al., 2012; Paugnam et al., 2016), aerosol microphysics (Forrister et al., 2015; Xie et al., 2018), and plume chemistry (Jaffe and Widger, 2011) are less understood. Recent field campaigns such as the NASA-NOAA FIREX-AQ campaign and Joint Fire Science's Fire Smoke and Model Evaluation Experiment (Prichard et al., 2019; Liu et al., 2019) have started unravelling some of the unknowns associated with smoke plume chemistry and aerosol physics, however, work is still needed that integrates observations with existing modeling smoke models. For example, shading from smoke aerosols can limit O_3 production in smoke plume despite wildfires emitting chemical precursors that are conducive for O_3 production (Verma et al., 2009). There are also questions surrounding the timescale it takes for NO_x to be converted into peroxyacetyl nitrate and then back to NO_x, which can be used to form O_3 (Alvarado et al., 2010). These are just a few of the many questions that needs to be addressed regarding smoke plume chemistry.

Properly evaluating fire plume rise models also continues to be a challenging proposition.

There are a limited number of observational datasets that measure the plume height and properties, while simultaneously constraining surface fire characteristics, such as the fire heat flux, burned area, and fuel consumption. Incomplete observational datasets makes it difficult to disentangle whether a simulated plume rise result is erroneous due to assumptions made within the model, or if errors stem from the model inputs, *e.g.,* fire area and heat fluxes (Val Martin et al., 2012).

Finally, work is also needed to better project future fire behavior and emissions. Outside of coupled fire-atmosphere models, most smoke modeling frameworks either use a persistence assumption (smoke today will be the same as smoke yesterday) or scale current fire heat fluxes and emissions using a diurnal curve. Therefore, most smoke models are unable to account for weather-driven fire effects on the plume dynamics. Recent studies have indicated that climate change is now impacting how some fires behave during the nighttime (Chiodi et al., 2021), which could further limit the usefulness of diurnal scaling techniques. While running a coupled fire-atmosphere model for every wildfire may not be practical with today's computing resources, new approaches could be developed to project future fire intensity based forecasted weather conditions.

As we head further into the future, our ability to monitor fires will continue to improve as remote sensing products and their post-processing algorithms become more sophisticated. New and exciting new tools are emerging that synthesizes remote sensing products with machine learning techniques. These sorts of tools can provide detailed fire information at a high spatiotemporal resolution, therefore reducing some of the uncertainties described earlier in this chapter (Farguell et al., 2021). Such tools will be critical for providing accurate inputs into smoke modeling frameworks. It is expected that these emerging technologies, combined with

851 data assimilation and improved computational resources will play an increasingly important rule
852 towards improving the representation of smoke transport and dispersion within smoke model.
853
854

Figures and Tables:

Table 1. List of commonly used smoke modeling frameworks for research and operational-based applications. The scale column are loose approximations of scales most appropriate for the listed model framework. Dashes within a column denote processes that are not accounted for. Gray shading intensity refers to the degree that specific processes are resolved where red is prescribed, yellow refers to processes that are parameterized, and green refers to explicitly resolve and/or parameterized and coupled.

Model	Model type	Scale	Fire Activity	Plume	Meteorology	Aerosol Physics	Chemistry
VSMOKE[1]	Gaussian	100-10,000m	Prescribed	Parameterized	Parameterized	-	Combustion only, smoke treated as passive tracer
SASEM[2]	Gaussian	100-10,000m	Prescribed	Parameterized	Parameterized	-	Combustion only, smoke treated as passive tracer
CALPUFF[3]	Puff model	1-1000 km	Prescribed	Parameterized	Parameterized	Parameterized	Parameterized
HYSPLIT[4]	Puff model	1-1000 km	Prescribed	Parameterized	Uncoupled	Parameterized	Parameterized
HYSPLIT[4]	LPDM	1-1000 km	Prescribed	Parameterized	Uncoupled	Parameterized	Parameterized
FLEXPART[5]	LPDM	1-1000 km	Prescribed	Parameterized	Uncoupled	Parameterized	Parameterized
STILT[6]	LPDM	1-1000 km	Prescribed	Parameterized	Uncoupled	Parameterized	Parameterized
DAYSMOKE[7]	Hybrid	1-10km	Parameterized	Parameterized	Parameterized or uncoupled	-	Combustion only, smoke treated as passive tracer
CMAQ-BlueSky[8]	Eularian	1-1000 km	Prescribed	Parameterized	Uncoupled	Parameterized	Parameterized
WRF-CHEM[9]	Eularian	1-1000 km	Prescribed	Parameterized	Resolved	Parameterized & coupled	Parameterized & coupled
GEOS-CHEM[10]	Eularian	"global"	Prescribed	Parameterized	Uncoupled	Parameterized	Parameterized
WRF-FIRE[11]	Coupled	100m-1000 km	Parameterized	Resolved	Resolved	-	Combustion only, smoke treated as passive tracer
WRF-SFIRE[12]	Coupled	100m-1000 km	Parameterized	Resolved	Resolved	Parameterized & coupled	Parameterized & coupled
WFDS[13]	Coupled	1m-1km	Resolved	Resolved	Resolved	-	Combustion only, smoke treated as passive tracer
HIGRAD-FIRETEC[14]	Coupled	1m-1km	Resolved	Resolved	Resolved	-	Combustion only, smoke treated as passive tracer

1. Lavdas (2006), 2. Sestak and Fiebau (1988), 3. Scire et al. (2000), 4. Draxler and Hess (1997), 5. Stohl and Thomson (1999), 6. Lin et al. (2003), 7. Achtemeir et al. (2011), 8. Larkin et al. (2009), 9. Grell et al. (2005), 10. http://acmg.seas.harvard.edu/geos/, 11. Coen et al. (2013), 12. Mandel et al. (2011), 13. Mell et al. (2007), 14. Linn and Cunningham (2005)

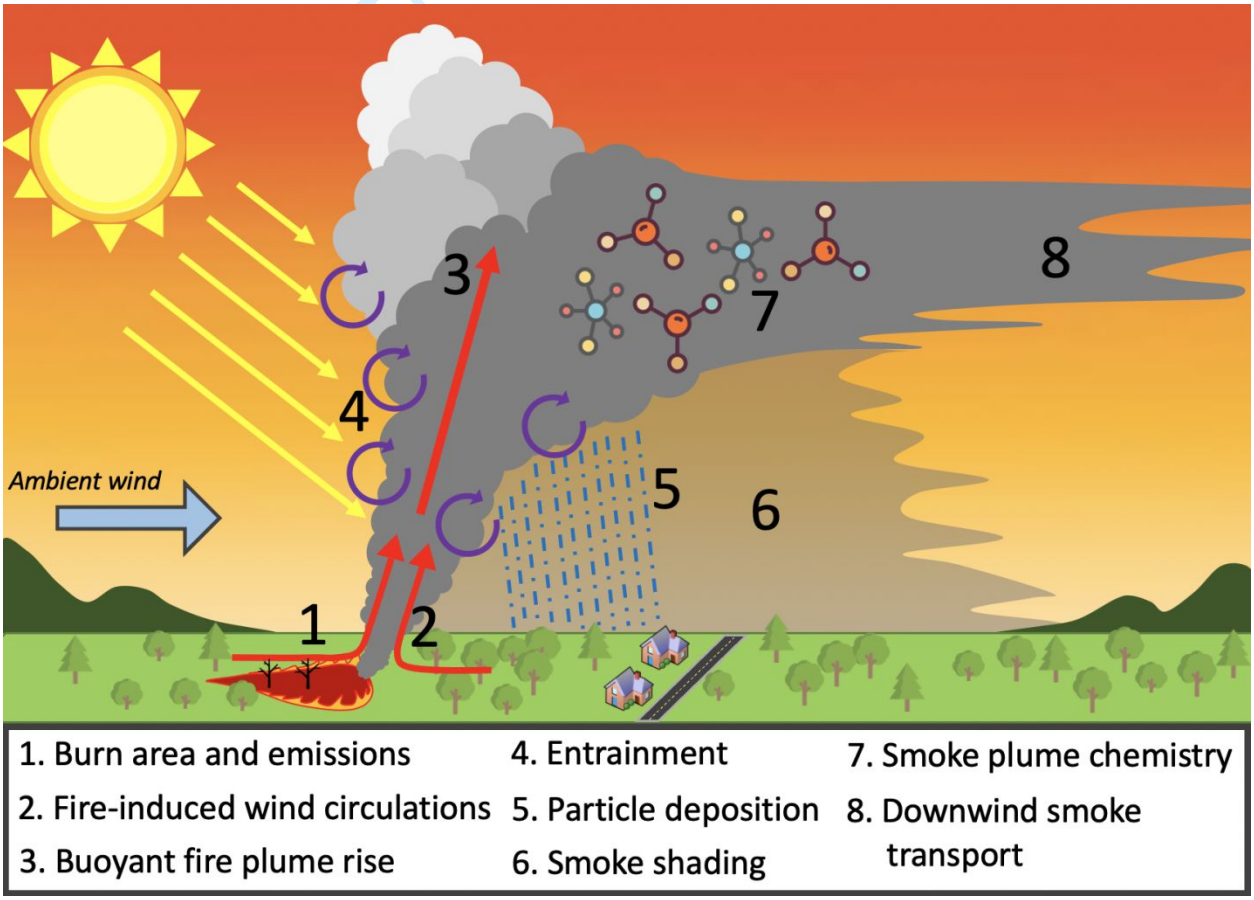

Figure 1. A schematic of important smoke transport processes. Definitions and details of these processes can be found in the chapter text.

907

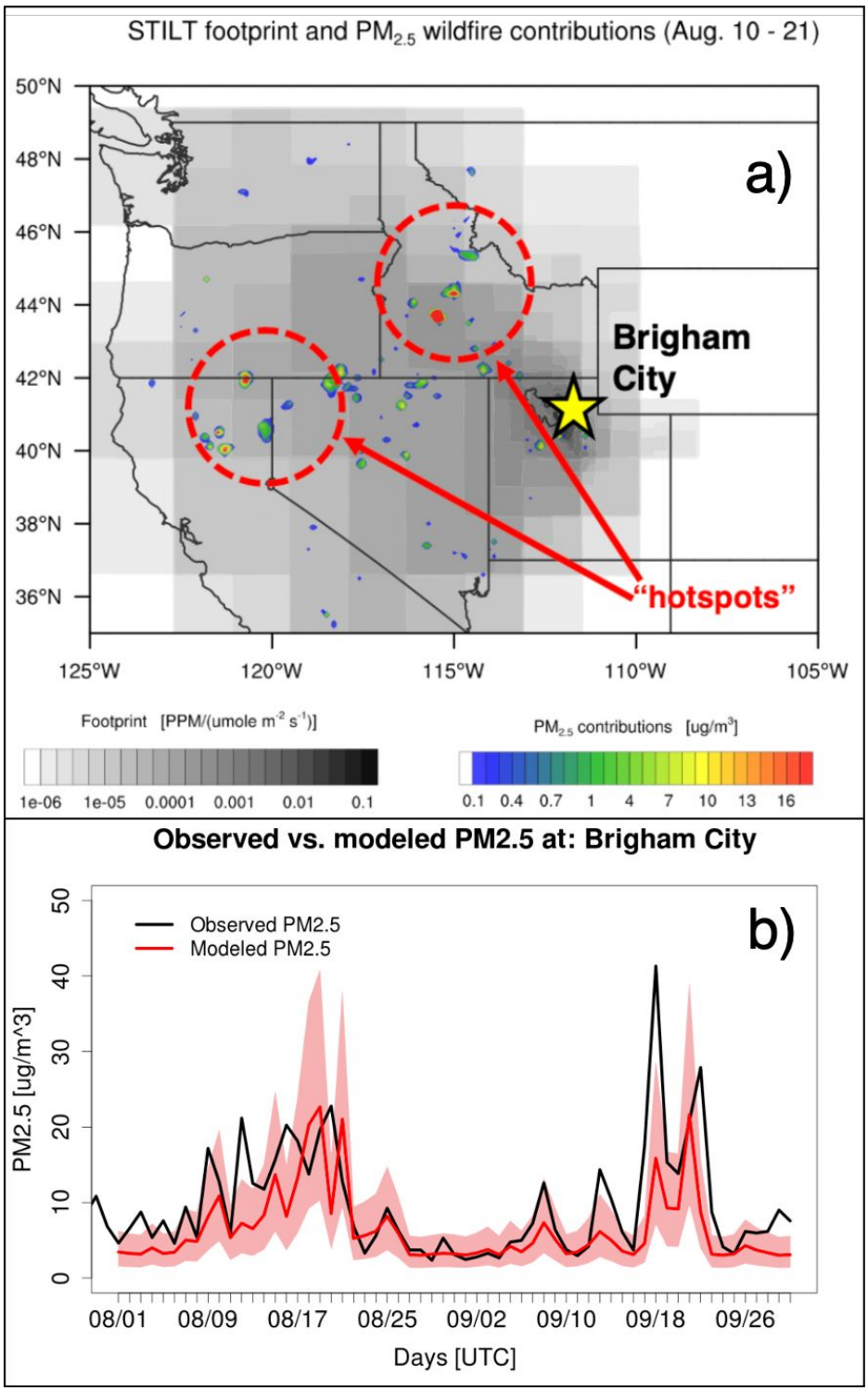

908

909 Figure 2. (a) STILT footprint (gray), which highlights backward trajectory transport pathways
910 averaged between August 10-21, 2012. $PM_{2.5}$ contributions from wildfires towards Brigham City
911 are shown by the color-filled contours. (b) Observed vs. modeled $PM_{2.5}$ concentrations at
912 Brigham City, UT for an episodic smoke event (fall 2012) with model uncertainties (+/-1σ)
913 related to transport errors are shaded as pink.

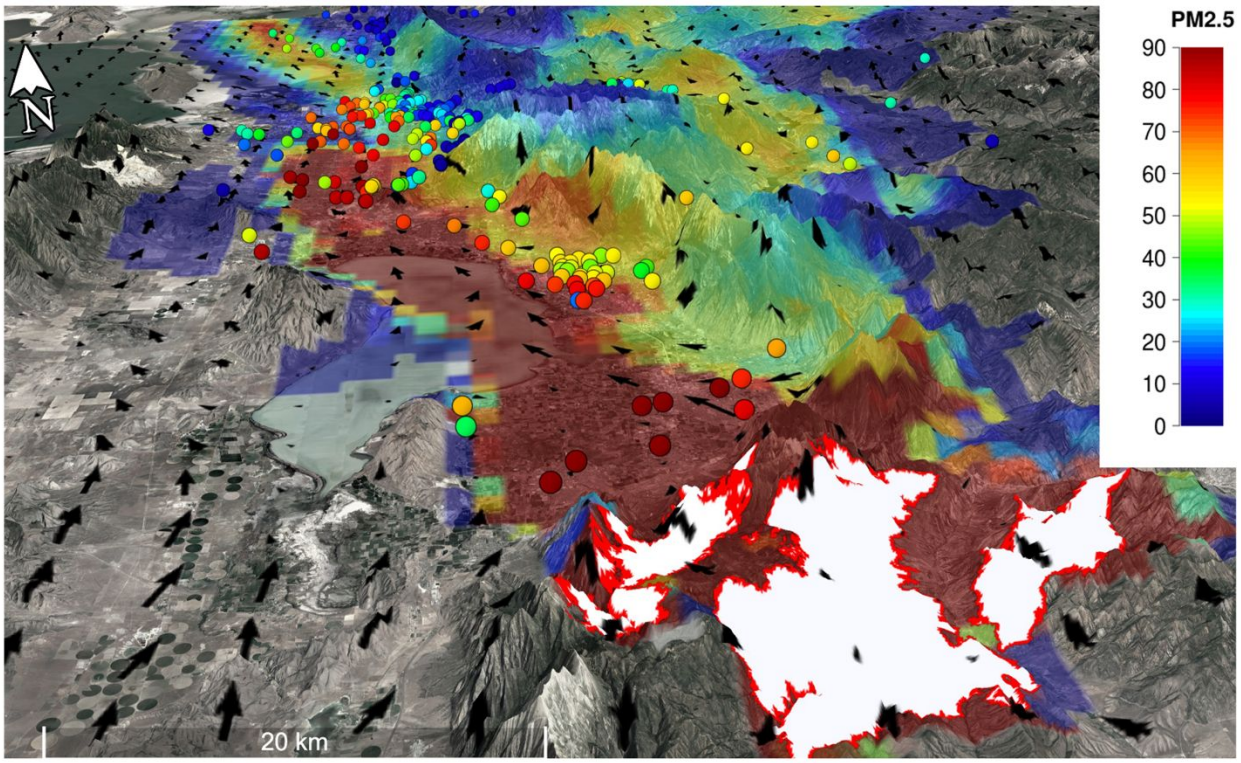

Figure 3. WRF-SFIRE-simulated and observed $PM_{2.5}$ concentrations for the Pole Creek and Bald Mountain fire on September 15th, 2018. Simulated smoke concentrations are represented by the color-filled contours, while observed $PM_{2.5}$ concentrations are denoted by the color-filled circles. All $PM_{2.5}$ concentrations displayed here are in units of $\mu g\ m^{-3}$. The white polygons in the lower right represent model-estimated burned areas, while the black arrows represent simulated near-surface winds.

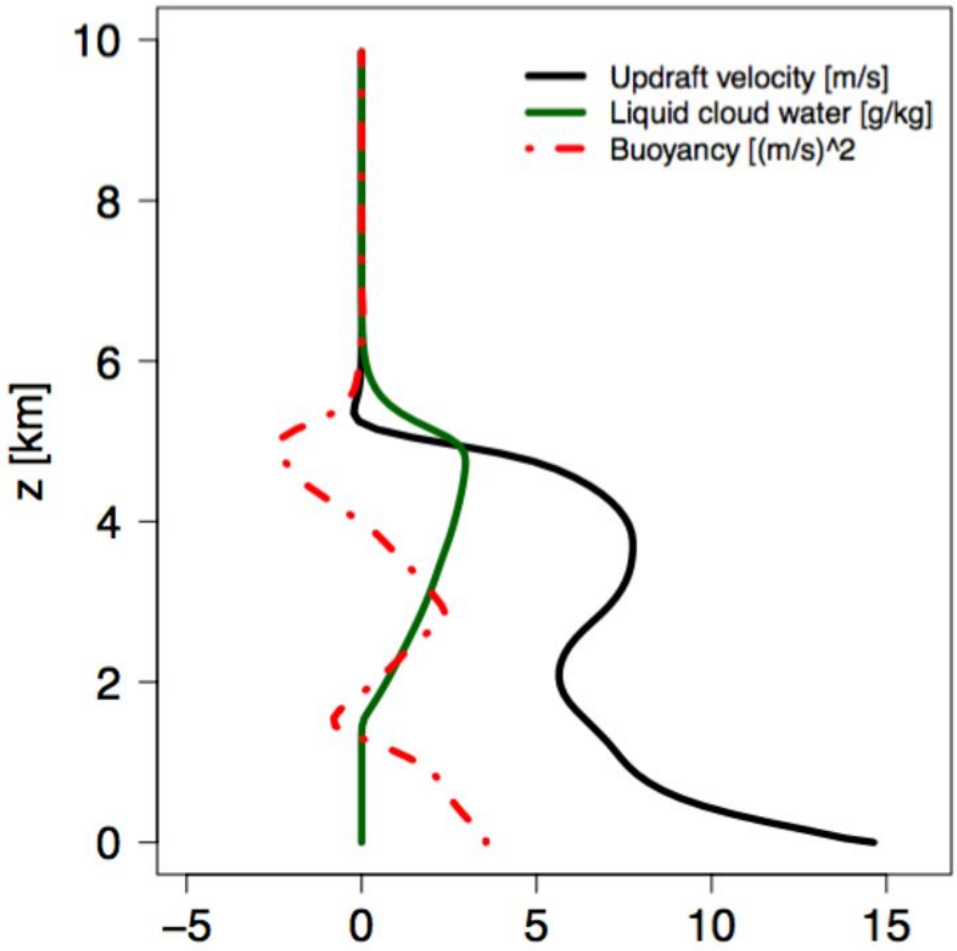

Figure 4. Plume rise simulation generated from the Freitas plume model for the 2012 Dry Creek Fire in Alaska.

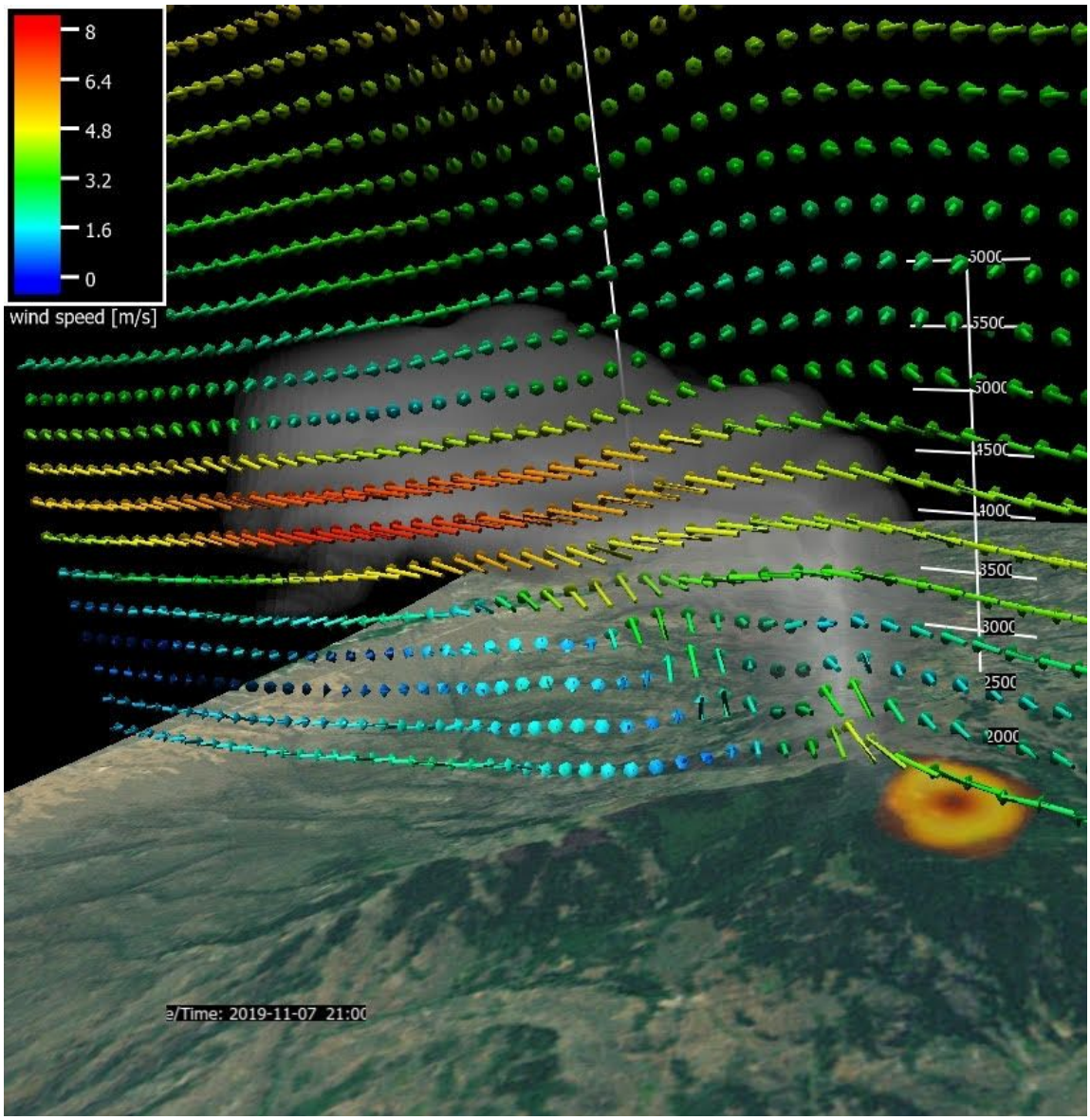

Figure 5. WRF-SFIRE simulated wildfire plume rise for the Anabella Reservoir prescribed burn. Warm-colored surface contours represent the modeled burn area, while the vectors represent simulated cross-sectional winds. Smoke is denoted by the transparent gray isosurface.

978 **References:**
979
980 Achtemeier, G. L., S. A. Goodrick, Y. Liu, F. Garcia-Menendez, Y. Hu, and M. T. Odman
981 (2011), Modeling smoke plume rise and dispersion from southern United States prescribed burns
982 with daysmoke. *Atmosphere*, 2, 358–388.
983
984 Ahmadov, R., G. Grell, E. James, S. Freitas, G. Pereira, I. Csiszar, et al. (2017). A
985 high-resolution coupled meteorology-smoke modeling system HRRR-Smoke to simulate air
986 quality over the CONUS domain in real time. *Geophysical Research Abstracts*, 19, 10841.
987
988 Akagi, S. K., R. J. Yokelson, C. Wiedinmyer, M. J. Alvarado, J. S. Reid, T. Karl, J. D. Crounse,
989 and P. O. Wennberg (2011), Emission factors for open and domestic biomass burning for use in
990 atmospheric models. *Atmos. Chem. Phys.*, 11, 4039–4072.
991
992 Alvarado, M. J. and Coauthors (2010), Nitrogen oxides and PAN in plumes from boreal fires
993 during ARCTAS-B and their impact on ozone: an integrated analysis of aircraft and satellite
994 observations. *Atmos. Chem. Phys.*, 10, 9739–9760.
995
996 Andreae, M.O., Merlet, P., 2001. Emission of trace gases and aerosols from biomass
997 burning. *Glob. Biogeochem. Cycles*, 15, 955–966.
998
999 Andreae, M. O., D. Rosenfeld, P. Artaxo, A. A. Costa, G. P. Frank, K. M. Longo and M. A. F.
1000 Silva-Dias (2004), Smoking rain clouds over the Amazon. *Science*, 303(5662), 1337–1342.
1001
1002 Archibald, A. T., M. E. Jenkin, and D. E. Shallcross (2010), An isoprene mechanism
1003 intercomparison. *Atmos. Environ.*, 44, 5356–5364.
1004
1005 Baker, K., and Coauthors (2018), Photochemical model evaluation of 2013 California wild fire
1006 air quality impacts using surface, aircraft, and satellite data. *Science of the Total Environment*,
1007 637, 1137–1149.
1008
1009 Banta R. M., L. D. Olivier, E. T. Holloway, R. A. Kropfli, B. W. Bartram, R. E. Cupp, and M. J.
1010 Post (1992), Smoke-column observations from two forest fires using Doppler lidar and Doppler
1011 radar. *J. Applied Meteorology*, 31, 1328–1349.
1012
1013 Barnes, J. E. and D. J. Hofmann, (1997), Lidar measurements of stratospheric aerosol over
1014 Mauna Loa Observatory. *Geophys. Res. Lett.*, 24, 1923–1926.
1015
1016 Battye, W., and R. Battye (2002), Final Report: Development of emissions inventory methods
1017 for wildland fire. EPA. https://www.epa.gov/ttn/chief/ap42/ch13/related/firerept.pdf.
1018
1019 Bauer, S.E., and S. Menon (2012). Aerosol direct, indirect, semidirect, and surface albedo effects
1020 from sector contributions based on the IPCC AR5 emissions for preindustrial and present-day
1021 conditions. J. Geophys. Res., 117, 1–15.
1022
1023 Bey, I., D. J. Jacob, R. M. Yantosca, J. A. Logan, B. D. Field, A. M. Fiore, and M .G. Schultz,

(2001). Global modeling of tropospheric chemistry with assimilated meteorology: Model description and evaluation. *J. Geophys. Res.*, 106(D19), 23073–23095.

Brey, S. J., and E. V. Fischer (2016), Smoke in the city: How often and where does smoke impact summertime ozone in the United States? *Environ. Sci. Techn.*, 50, 1288–94.

Briggs, G. A. (1975), Plume Rise Predictions. Lectures on Air Pollution and Environmental Impact Analyses. 72-73. *American Meteorological Society*, Boston, MA, USA.

Brown J. K., L. S. Bradshaw (1994), Comparisons of particulate emissions and smoke impacts from presettlement, full suppression, and prescribed natural fire periods in the Selway-Bitterroot Wilderness. *International Journal of Wildland Fire*, 4(3), 143–155.

Burling, I. R., R. J. Yokelson, D. W. T. Griffith, T. J. Johnson, P. Veres, J. M. Roberts, C. Warneke, S. P. Urbanski, J. Reardon, J., D. R. Weise, W. M. Hao, W. M., and J. de Gouw, (2010), Laboratory measurements of trace gas emissions from biomass burning of fuel types from the southeastern and southwestern United States. *Atmos. Chem. Phys.*, 10, 1115–11130.

Byun, D., and K. L. Schere (2006), Review of the governing equations, computational algorithms, and other components of the Models-3 Community Multiscale Air Quality (CMAQ) Modeling System. *Applied Mechanics Reviews*, 59, 51–77.

Chen, L.-W. A., H. Moosmüller, W. P. Arnott, J. C. Chow, J. G. Watson, R. A. Susott, R.E. Babbitt, C. E. Wold, E. N. Lincoln, W. M. Hao (2007), Emissions from laboratory combustion of wildland fuels: emission factors and source profiles. *Environ. Sci. Technol.*, 2, 4317–4325.

Chen, Y., Q, Li, J. T. Randerson, E. A. Lyons, R. A. Kahn, D. L. Nelson, and D. J. Diner (2009), The sensitivity of CO and aerosol transport to the temporal and vertical distribution of North American boreal fire emissions. *Atmos. Chem. Phys.*, 9, 6559–6580.

Chin, M., R. B. Rood, S.-J. Lin, J. F. Muller, and A. M. Thomspon (2000), Atmospheric sulfur cycle in the global model GOCART: Model description and global properties, *J. Geophys. Res.*, 105, 24671–24687.

Chiodi, A. M., B. E. Potter, and N. K. Larkin (2021), Multi-decadal change in Western US nighttime vapor pressure deficit. *Geophys. Res. Lett.*, 48, e2021GL092830.

Choi, Y-J, and H. J. S. Fernando (2007), Simulation of smoke plumes from agricultural burns: application to the San Luis/Rio Colorado airshed along the US/Mexico border. *Sci. Total Environ.*, 388(1–3), 270–289.

Christian, K., J. Wang, C. Ge, D. Peterson, E. Hyer, J. Yorks, and M. McGill (2019), Radiative forcing and stratospheric warming of pyrocumulonimbus smoke aerosols: First modeling results with multisensor (EPIC, CALIPSO, and CATS) views from space. *Geophys. Res. Lett.*, *46*, 10061–10071.

Coen, J. L., M. Cameron, J. Michalakes, E. G. Patton, P. J. Riggan, and K. M. Yedinak (2013), WRF-Fire: Coupled Weather -Wildland Fire Modeling with the Weather Research and Forecasting Model. *J. Appl. Meteor. Climat.*, 52, 1, 16–38.

Cunningham, P., S. L. Goodrick, M. Y. Hussaini, and R. R. Linn (2005), Coherent vortical structures in numerical simulations of buoyant plumes from wildland fires. *International Journal of Wildland Fire,* 14, 61–75.

Cunningham, P., and S. L. Goodrick (2012), High-Resolution numerical models for smoke transport in plumes from wildland fires. Remote Sensing and Modeling Applications to Wildland Fires. Springer-Verlag, Tsinghua University Press, pp. 74–88.

Decker, Z. C., and Coauthors (2021), Nighttime and daytime dark Oxidation Chemistry in Wildfire Plumes: An Observation and Model Analysis of FIREX-AQ Aircraft Data, *Atmos. Chem. Phys. Discuss.*, https://doi.org/10.5194/acp-2021-267.

Draxler, R. R., and G. D. Hess (1997), Description of the HYSPLIT_4 modeling system. NOAA Technical Memorandum ERL, ARL-224.

Elguindi, N., H. Clark, C. Ordóñez, V. Thouret, J. Flemming, O. Stein, V. Huijnen, P. Moinat, A. Inness, V.-H. Peuch, A. Stohl, S. Turquety, G. Athier, J.-P. Cammas, and M. Schultz (2020), Current status of the ability of the GEMS/MACC models to reproduce the tropospheric CO vertical distribution as measured by MOZAIC. *Geosci. Model Dev.*, 3, 501–518.

Emerson, E. W., A. L. Hodshire, H. M. DeBolt, K. R. Bilback, J. R. Pierce, G. R. McMeeking, and D. K. Farmer (2020), Revisiting particle dry deposition and its role in radiative effect estimates. *PNAS*, 117(42), 26076–26082.

Emmons, L. K., and Coathors (2010), Description and evaluation of the model for ozone and related chemical tracers, version 4 (MOZART-4). *Geosci. Model Dev.*, 3(1), 43–67.

Farguell, A., J. Mandel, J. Haley, D. V. Mallia, A. Kochanski, and K. Hillburn (2021), Machine learning estimation of fire arrival time from level-2 active fire satellite data. *Remote Sensing*, 13(11), 2203.

Finlayson-Pitts, B.J., and J. N. Pitts, (1986), Atmospheric Chemistry: Fundamentals and Experimental Techniques. John Wiley and Sons, New York, NY.

Forrister, H., J. Liu, E. Scheuer, J. Dibb, L. Ziemba, K. L. Thornhill, et al. (2015). Evolution of brown carbon in wildfire plumes. *Geophys. Res. Lett.*, 42, 4623–4630.

Freitas, S. R., K. M. Longo, R. Chatfield, D. Latham, M. A. F. S. Dias, M. O. Andreae, E. Prins, J. C. Santos, R. Gielow, and J. A. Carvalho (2007), Including the sub-grid scale plume rise of vegetation fires in low resolution atmospheric transport models. *Atmos. Chem. Phys.*, 7, 3385–3398.

Freitas, S. R., K. M. Longo, J. Trentmann, and D. Latham (2010), Technical note: Sensitivity of 1-D smoke plume rise models to the inclusion of environmental wind drag. *Atmos. Chem. Phys*., 10, 585–594.

Fromm, M., D. T. Lindsey, R. Servranckx, G. Yue, T. Trickl, R. Sica, P. Doucet, and S. Godin-Beekmann (2010), The untold story of the pyrocumulonimbus. *BAMS*, 91(9), 1193–1210.

Giglio, L. (2007), Characterization of the tropical diurnal fire cycle using VIRS and MODIS observations. *Remote Sens. Environ*., 108(4), 407–421.

Goodrick, S. L., G. L. Achtemeier, N. K. Larkin, Narasimhan, Y. Liu, T. Strand (2012), Modelling smoke transport from wildland fires: a review, *Int. J. Wildland Fire*, http://dx.doi.org/10.1071/WF11116.

Grell G. A., S. E. Peckham, S. McKeen, R. Schmitz, G. Frost, W. C. Skamarock, and B. Eder (2005), Fully coupled 'online' chemistry within the WRF model. *Atmospheric Environment*, 39, 6957–6975.

Grell, G., S. R. Freitas, M. Stuefer, and J. Fast (2011), Inclusion of biomass burning in WRF-Chem: impact of wildfires on weather forecasts. *Atmos. Chem. Phys. Discuss.*, 10, 30 613–30 650.

Hodzic, A., S. Madronich, B. Bohn, S. Massie, L. Menut and C. Wiedinmyer (2007), Wildfire particulate matter in Europe during summer 2003: meso-scale modeling of smoke emissions, transport and radiative effects. *Atmos. Chem. Phys. Discuss.*, 7(2), 4705–4760.

Haikerwal, A., F. Reisen, M. R. Sim, M. J. Abramson, C. P. Meyer, F. H. Johnston, and M. Dennekamp (2015), Impact of smoke from prescribed burning: Is it a public health concern? *J. Air and Waste Manage. Assoc.*, 65, 592–598.

Hyer, E. J. and B. N. Chew (2010), Aerosol transport model evaluation of an extreme smoke episode in Southeast Asia. *Atmos. Environ.*, 44, 1422–1427.

Jackson W. A., G. L. Achtemeier, and S. L. Goodrick (2007); A technical evaluation of mmoke dispersion from the Brush Creek Prescribed fire and the impacts on Asheville, North Carolina. Available at: http://www.nifc.gov/smoke/documents/Smoke_Incident_Impacts_Asheville_NC.pdf.

Jaffe, D., I. Bertschi, L. Jaegle, P. Novelli, J. S. Reid, H. Tanimoto, R. Vingarzan, and D. L. Westphal (2004), Long-range transport of Siberian biomass burning emissions and impact on surface ozone in western North America. *Geophys. Res. Lett.*, 31, L16106.

Jaffe, D. A., and N. L. Wigder (2012), Ozone production from wildfires: A critical review. *Atmos. Environ.*, 51, 1–10.

Jain R, J. Vaughan, H. Kyle, C. Ramosa, C. Clalborn, S. Maarten, M. Schaaf, and B. Lamb (2007), Development of the ClearSky smoke dispersion forecast system for agricultural field burning in the Pacific Northwest. *Atmos. Environ.*, 41, 6745–6761.

Kalnay, E. (2003), Atmospheric Modeling, Data Assimilation and Predictability. Cambridge University Press, 369 pp.

Kochanski, A. K., M. A. Jenkins, K. Yedinak, J. Mandel, J. Beezley, and B. Lamb (2016), Toward an integrated system for fire, smoke, and air quality simulations, *Int. J. Wildland Fire*, *25*, 558–568.

Kochanski, A. K., A. Fournier, and J. Mandel (2018), Experimental design of a prescribed burn instrumentation. *Atmosphere*, *9*, 296.

Kochanski, A. K., D. V. Mallia, M. Fearon, T. Brown, and J. Mandel (2019), Modeling wildfire smoke feedback mechanisms using a coupled fire-atmosphere model with a radiatively active aerosol scheme. *J. Geophys. Res.*, 124(16), 9099–9116.

Lahm, P. (2015), Wildfire, prescribed fire and the Clean Air Act: the latest challenges and opportunities. *6th International Fire Ecology and Management Congress: advancing ecology in fire management*, November 16–20, San Antonio, TX.

Latham, D. (1994), PLUMP: A one-dimensional plume predictor and cloud model for fire and smoke managers. *Gen. Tech. Rep. INT-GTR-314*, Intermt. Res. Stn., For. Serv., U.S. Dep. of Agric., Fort Collins, Colo

Lavdas, L. G. (1996), Program VSMOKE – users manual. USDA Forest Service, Southeastern Forest Experiment Station, General Technical Report SRS-6. (Macon GA)

Lareau, N. P. and C. B. Clements (2015), Cold Smoke: smoke-induced density currents cause unexpected smoke transport near large wildfires, *Atmos. Chem. Phys.*, *15*, 11513–11520.

Lareau, N. P. and C. B. Clements (2016), Environmental controls on pyrocumulus and pyrocumulonimbus initiation and development. *Atmos. Chem. Phys.*, 16, 4005–4022.

Lareau, N., and C. Clements, 2017: The mean and turbulent properties of a wildfire convective plume. *J. Appl. Meteor. Climatol.*, 56(8), 2289–2299.

Larkin, N. K., S. M. O'Neill, R. Solomon, S. Raffuse, T. Strand, D. C. Sullivan, and S. A. Ferguson (2009), The BlueSky Smoke Modeling Framework. *Int. J. Wildland Fire*, 18, 906–920.

Lee, H., S.-J. Jeong, O. Kalashnikova, M. Tosca, S.-W. Kim, and J.-S. Kug, (2018), Characterization of wildfire-induced aerosol emissions from the Maritime Continent peatland and Central African dry savannah with MISR and CALIPSO aerosol products. *J. Geophys. Res.*, 123, 3116–3125.

Lelieveld, J., J. S. Evans, M. Fnais, D. Giannadaki, and A. Pozzer (2015), The contribution of outdoor air pollution sources to premature mortality on a global scale. *Nature*, *525*, 367–384.

Leung, F.-Y. T., J. A. Logan, R. Park, E. Hyer, E. Kasischke, D. Streets, and L. Yurganov (2007), Impacts of enhanced biomass burning in the boreal forests in 1998 on tropospheric chemistry and the sensitivity of model results to the injection height of emissions. *J. Geophys. Res.-Atmos.*, 112, D10313.

Li, Y., M. J. Loretta, P. Liu, and J. O. Kaplan (2020), Trends and spatial shifts in lightning fires and smoke concentrations in response to 21st century climate over the national forests and parks of the western United States. *Atmos. Phys. Chem.*, 20, 8827–8838.

Lim, C. Y., and Coauthors (2019), Secondary organic aerosol formation from the laboratory oxidation of biomass burning emissions. *Atmos. Chem. Phys.*,19, 12797–12809.

Lindsey, D. T., and M. Fromm (2008), Evidence of the cloud lifetime effect from wildfire-induced thunderstorms. *Geophys Res. Lett.*, 35, L22809.

Linn R. R., J. Reisner, J. J. Colmann, and J. Winterkamp (2002), Studying wildfire behavior using FIRETEC. *Int. J. Wildland Fire*, *11*, 233–246.

Linn, R. R., and P. Cunningham (2005), Numerical simulations of grass fires using a coupled atmosphere-fire model: basic fire behavior and dependence on wind speed. *J Geophy. Res.*, 110, D13107.

Liu, X., P.-L. Ma, H. Wang, S. Tilmes, B. Singh, R. C. Easter, S. J. Ghan, and P. J. Rasch (2016b), Description and evaluation of a new 4-mode version of Modal Aerosol Module (MAM4) within version 5.3 of the Community Atmosphere Model. *Geosci. Model. Dev.*, 9, 505–522.

Liu, Y., S. Goodrick, G. Achtemeier, W. Jackson, J. Qu, and W. Wang (2009), Smoke incursions into an urban area: simulation of a Georgia prescribed burn. *Int. J. Wildland Fire*, 18(3), 336–348.

Liu, Y. Q., G. L. Achtemeier, S. L. Goodrick, and W. A. Jackson (2010), Important parameters for smoke plume rise simulation with Daysmoke. *Atmospheric Pollution Research*, 1, 250–259.

Liu, J. C., and Coauthors (2016a), Particulate air pollution from wildfires in the Western U.S. under climate change. Climate Change, 138, 655–666.

Liu Y., A. Kochanski, K. Baker, W. Mell, R. Linn, R. Paugam, J. Mandel, A. Fournier, M. Jenkins, S. Goodrick, G. Achtemeier, F. Zhao, R. Ottmar, N. French, N. Larkin, T. Brown, A. Hudak, M. Dickinson, B. Potter, C. Clements, S. P. Urbanski, S. Prichard, A. Watts, and D. McNamara (2019), Fire behavior and smoke modelling: model improvement and measurement needs for next-generation smoke research and forecasting systems. International Journal of Wildland Fire 28, 570-588.

Lobert, J. (1991), Experimental evaluation of biomass burning emissions: nitrogen and carbon containing compounds, in: Global Biomass Burning: Atmospheric, Climatic and Biospheric Implications. MIT Press, Cambridge, MA, pp. 289– 304.

Loughner, C., B. Fasoli, A.F. Stein, and J.C. Lin (2021), Incorporating features from the Stochastic Time-Inverted Lagrangian Transport (STILT) model into the Hybrid Single-Particle Lagrangian Integrated Trajectory (HYSPLIT) model: a unified dispersion model for time-forward and time-reversed applications, *J. Appl. Meteor. Climat.*, 60, 799–810.

Lu, Z., and I. N. Sokolik (2013), The effect of smoke emission amount on changes in cloud properties and precipitation: A case study of Canadian boreal wildfires of 2007. *J. Geophys. Res.*, 118, 11777–11793.

Luderer, G., J. Trentmann, T. Winterrath, C. Textor, M. Herzog, H.-F. Graf, and M. O. Andreae (2006), Modeling of biomass smoke injection into the lower stratosphere by a large forest fire (Part II): sensitivity studies. *Atmos. Chem. Phys*. 6, 5261–5277.

Mallia, D. V., J. C. Lin, S. Urbanski, J. Ehleringer, and T. Nehrkorn (2015), Impacts of upwind wildfire emissions on CO_2, CO, and $PM_{2.5}$ concentrations in Salt Lake City, Utah. *J. Geophys. Res.*, 120(1), 147–166.

Mallia, D. V., A. Kochanski, S. Urbanski, and J. C. Lin (2018), Optimizing smoke and plume rise modeling approaches at local scales. *Atmosphere*, 9, 116.

Mallia, D. V., A. Kochanski, S. Urbanski, J. Mandel, A. Farguell, and S. Krueger (2020a), Incorporating a canopy parameterization within a coupled fire-atmosphere model to improve a smoke simulation for a prescribed burn. *Atmosphere*, 11(8), 832.

Mallia, D. V., A. K. Kochanski, K. E. Kelly, R. Whitaker, W. Xing, L. Mitchell, A. Jacques, A. Farguell, J. Mandel, P.-E. Gaillardon, T. Becnel, and S. Krueger (2020b), Evaluating wildfire smoke transport within a coupled fire-atmosphere model using a high-density observation network for an episodic smoke event along Utah's Wasatch Front. *J. Geophys. Res.*, 125, e2020JD032712.

Mandel, J., J. D. Beezley, A. K. Kochanski (2011), Coupled atmosphere-wildland fire modeling with WRF 3.3 and SFIRE 2011. *Geosci. Model Devel.*, *4*, 591–610.

McMeeking G. R., S. M. Kreidenweis, S. Baker, C. M. Carrico, J. C. Chow, J. L. Collett, W. M. Hao, A. S. Holden, T. W. Kirchstetter, W.C. Malm, H. Moosmüller, A. P. Sullivan, C. E. Wold (2009), Emissions of trace gases and aerosols during the open combustion of biomass in the laboratory. *J. Geophys. Res.-Atmos.*, 114, D19210.

Mell, W., M. A. Jenkins, J. Gould, and P. Cheney P (2007), A physics-based approach to modeling grassland fires. *Int. J. Wildland Fire*, 16, 1–22.

O'Neill, S.M., N. K Larkin, J. Hoadley, G. Mills, J. Vaughan, R. Draxler, G. Roph, M. Ruminski, and S. A. Ferguson (2008), Regional real-time smoke prediction systems. Wildland Fires and Air Pollution, A. Bytnerowicz et al., Eds., Developments in Environmental Science Series, Vol. 8, Elsevier, 499-534.

Paugam, R., M. Wooster, S. Freitas, and M. Val Martin (2016), A review of approaches to estimate wildfire plume injection height within large-scale atmospheric chemical transport model. *Atmos. Chem. Phys.*, 16, 907–925.

Paulot, F., J. D. Crounse, H. G. Kjaergaard, J. H. Kroll, J. H. Seinfeld, and P. O. Wennberg (2009), Isoprene photooxidation: new insights into the production of acids and organic nitrates. *Atmos. Chem. Phys.*, 9, 1479–1501.

Peng, Q., and Coauthors (2020), HONO emissions from western U.S. wildfires provide dominant Radical source in fresh wildfire smoke. *Environ. Sci. Technol.*, 54(10), 5954–5963.

Peterson, D. A., J. R. Campbell, E. J. Hyer, M. D. Fromm, G. P. Kablick, J. H. Cossuth, and M. T. DeLand (2018), Wildfire-driven thunderstorms cause a volcano-like stratospheric injection of smoke. *npj Climate and Atmospheric Science*, 1(1), 30.

Peterson, J. and Coauthors (2020), NWCG Smoke Management Guide for Prescribed Fire. *National Wildfire Coordinating Group*. PMS 420-3.

Pfister, G. G., C. Wiedinmyer, and L. K. Emmons (2008), Impacts of the fall 2007 California wildfires on surface ozone: Integrating local observations with global model simulations. *Geophys. Res. Lett.*, 35.

Pfister, G. G., J. Avise, C. Wiedinmyer, D. P. Edwards, L. K. Emmons, G. D. Diskin, J. Podolske, and A. Wisthaler (2011), CO source contribution analysis for California during ARCTAS-CARB. *Atmos. Chem. Phys.*, 11(15), 7515–7532.

Pharo J. A., L. G. Lavdas and P. M. Bailey PM (1976), Smoke Transport and Dispersion. In 'Southern Forestry and Smoke Management Guidebook'. (Ed. HE Mobley) USDA Forest Service, Southeastern Research Station, General Technical Report SE-10, Chap. 5, pp. 45–55.

Powers, J., and Coauthors (2017), The Weather Research and Forecasting Model: Overview, system efforts, and future direction. *Bull. Amer. Meteor.*, 98(8), 1717–1737.

Prichard, S. and Coauthors (2019), The fire and smoke model evaluation experiment—a plan for integrated, large fire–atmosphere field campaigns. *Atmosphere*, 10(2), 66.

Raffuse, S. M., K. J. Craig, N. K. Larkin, T. T. Strand, D. C. Sullivan, N. J. M. Wheeler, and R. Solomon (2012), An Evaluation of modeled plume injection height with satellite-derived observed plume height. *Atmosphere*, 3, 103–123.

Rappold, A. G., N. L. Fann, J. Crooks, J. Huang, W. E. Cascio, R. B. Devlin, D. Diaz-Sanchez

(2014), Forecast-based interventions can reduce the health and economic burden of wildfires. *Environ. Sci. & Techn.*, 48(8), 10571–10579.

Robock, A. (1988), Enhancement of Surface Cooling Due to Forest Fire Smoke, *Science*, *242*, 911–913.

Robock, A. (1991), Surface cooling due to forest fire smoke, *J. Geophys. Res.*, 96, 2156–2202.

Robock, A. (2000), Volcanic eruptions and climate. *Rev. Geophys.*, 38, 191–219.

Rothermel R (1972), A mathematical model for predicting fire spread in wildland fuels. Technical Report Research Paper INT 115, USDA Forest Service, Intermountain Forest and Range Experiment Station, Ogden, UT, 1-46.

Saylor, R. D., D. Barry, P. Lee, D. Tong, L. Pan and B. B. Hicks (2019), The particle dry deposition component of total deposition from air quality models: right, wrong or uncertain? *Tellus B: Chemical and Physical Meteorology*, 71:1, 1550324.

Scire, J. S., D. G. Strimaitis, and R. J. Yamartino (2000), A user's guide for the CALPUFF Dispersion Model (version 5.0). edited, pp. 521-521, Earth Tech, Inc, Concord, MA.

Segal, M. and R. W. Arritt (1992), Nonclassical mesoscale circulations caused by surface sensible heat-flux gradients, *B. Am. Meteor. Soc.*, 73, 1593–1604.

Sessions, W. R., H. E. Fuelberg, R. A. Kahn, and D. M. Winker (2011), An investigation of methods for injecting emissions from boreal wildfires using WRF-Chem during ARCTAS. *Atmos. Chem. Phys.*, 11(12), 5719–5744.

Sestak, M. L. and A. R. Riebau (1988), SASEM, Simple approach smoke estimation model. US Bureau of Land Management, Technical Note 382.

Shin, H. H., and S.-Y. Hong (2015), Representation of the subgrid-scale turbulent transport in convective boundary layers at gray-zone resolutions. *Mon. Wea. Rev.*, 143, 250–271.

Sofiev, M., T. Ermakova, and R. Vankevich (2012), Evaluation of the smoke-injection height from wild-land fires using remote-sensing data. *Atmos. Chem. Phys.*, 12, 1995–2006.

Sofiev, M., R. Vankevich, T. Ermakova, and J. Hakkarainen (2013), Global mapping of maximum emission heights and resulting vertical profiles of wildfire emissions. *Atmos. Chem. Phys.*, 13, 7039–7052.

Spracklen, D. V., L. J. Mickley, J. A. Logan, R. C. Hudman, R. Yevich, M. D. Flannigan, and A. L. Westerling (2009), Impacts of climate change from 2000 to 2050 on wildfire activity and carbonaceous aerosol concentrations in the western United States. *J. Geophys. Res.*, 114, D20301.

Solomos, S., V. Amiridis, P. Zanis, E. Gerasopoulos, F. I. Sofiou, T. Herekakis, J. Brioude, A. Stohl, R. Kahn, and C. Kontoes (2015), Smoke dispersion modeling over complex terrain using high resolution meteorological data and satellite observations - The Fire Hub platform, *Atmos. Environ.*, 119, 348–361.

Taylor, G. I. (1922), Diffusion by continuous movements. Proc. London Math. Soc., 20, 196–212.

Tanimoto, H., K. Matsumoto, M. Uematsu, (2008), Ozone-CO correlations in Siberian wildfire plumes observed at Rishiri Island. *Sola*, 4, 65–68.

Trentmann, J., G. Luderer, T. Winterrath, M. D. Fromm, R. Servranckx C. Textor M. Herzog G.-F. Graf, and M. O Andreae (2006), Modeling of biomass smoke injection into the lower stratosphere by a large forest fire (Part I): reference simulation. *Atmos. Chem. Phys.*, 6, 5247–5260.

Turquety, S., J. A. Logan, D. J. Jacob, R. C. Hudman, F. Y. Leung, C. L. Heald, R. M. Yantosca, D. Wu, L. K. Emmons, D. P. Edwards, and G. W. Sachse (2007), Inventory of boreal fire emissions for North America in 2004: Importance of peat burning and pyroconvective injection. *J. Geophys. Res.-Atmos.*, 112, D12S03.

Urbanski, S. P., W. M. Hao, and B. Nordgren (2011), The wildland fire emission inventory: western United States emission estimates and an evaluation of uncertainty. *Atmos. Chem. Phys.*, 11, 12973–1300.

Urbanski, S. (2014), Wildland fire emissions, carbon, and climate: Emission factors. *Forest Ecol. Manage.*, 317, 51–60.

Urbanski, S. P., M. C. Reeves, R. E. Corley, W. M. Hao, and R. P. Silverstein (2017), Missoula Fire Lab Emission Inventory (MFLEI) for CONUS. Fort Collins, CO: Forest Service Research Data Archive. https://doi.org/10.2737/RDS-2017-0039

Val Martin, N., R. Kahn, J. A. Logan, R. Paugnam, M. Wooster, and C. Ichoku (2012), Space-based observational constraints for 1-D fire smoke plume-rise models. *J. Geophys. Res.*, 117, D22204.

van der Werf, G. R., J. T. Randerson, L. Giglio, G. J. Collatz, M. Mu, P. S. Kasibhatla and T. T. v. Leeuwen (2010), Global fire emissions and the contribution of deforestation, savanna, forest, agricultural, and peat fires (1997–2009). *Atmos. Chem. Phys.*, 10(23), 11707–11735.

Walcek, C. J. (2002), Effects of wind shear on pollution dispersion. *Atmos. Environ.*, 36, 511–517.

Walter, C., S. R. Freitas, C. Kottmeier, I. Kraut, D. Rieger, H. Vogel, and B. Vogel (2016), The importance of plume rise on the concentrations and atmospheric impacts of biomass burning aerosol. *Atmos. Chem. Phys.*, 16(14), 9201–9219.

Wiedinmyer, C., S. K. Akagi, R. J. Yokelson, L .K. Emmons, J. A. Al-Saadi, J. J. Orlando, A. J. Soja (2010), The Fire INventory from NCAR (FINN): a high resolution global model to estimate the emissions from open burning. *Geosci. Moel Develop. Discuss.*, 3, 2439–2476.

Weisman, M. L., C. Davis, W. Wang, K. W. Manning, and J. B. Klemp (2008), Experiences with 0–36-h explicit convective forecasts with the WRF-ARW Model. *Wea. Forecasting*, 23, 407–437.

Westerling, A. L., H. G. Hidalgo, D. R. Cayan, and T. W. Swetnam (2006), Warming and earlier spring increases western U.S. forest fire activity. *Science*, 313, 940–943.

Wolfe, G. M., M. R. Marvin, S. J. Roberts, K. R. Travis and J. Liao (2016), The framework for 0-D atmospheric modeling (F0AM) v3.1, *Geosci. Model Dev.*, 9(9), 3309–3319.

Wotawa, G., M. Trainer (2000), The influence of Canadian forest fires on pollutant concentrations in the United States. *Science*, 288, 324–328.

Xie, M., M. D. Hays, and A. L. Holder (2017), Light-absorbing organic carbon from prescribed and laboratory biomass burning and gasoline vehicle emissions. *Scientific Reports*, 7, 7318.

Verma, S., and Coauthors (2009), Ozone production in boreal fire smoke plumes using observations from the Tropospheric Emission Spectrometer and the Ozone Monitoring Instrument. *J. Geophys. Res.*, 114, D02303.

Viegas, D. X. (1998), Convective processes in forest fires, in: Buoyant Convection in Geophysical Flows, edited by: Plate, E. J., Fedorovich, E. E., Viegas, D. X., and Wyngaard, J. C., Kluwer Academic Publishers, AA Dordrecht, The Netherlands, pp. 401–420

Yokelson, R., D. Griffith, and D. Ward (1996), Open-path Fourier transform infrared studies of large-scale laboratory biomass fires. *J. Geophys. Res.-Atmos.*, 101, 21067–21080.

Zaveri, R. A., R. C. Easter, J. D. Fast, and L. K. Peters (2008), Model for simulating aerosol interactions and chemistry (MOSAIC), J. *Geophys. Res.*, 113, D13204.

Zhang, L. M., S. L. Gong, J. Padro, L. Barrie (2001), A size-segregated particle dry deposition scheme for an atmospheric aerosol module. *Atmos. Environ.*, 35, 549–560.

Zhang, Y., J. Fan, T. Logan, Z. Li, and C. R. Homeyer (2019), Wildfire impact on environmental thermodynamics and severe convective storms. *Geophys. Res. Lett*., 46, 10082–10093.

Zou, Y. and Coathors (2019). Machine learning-based integration of high-resolution wildfire smoke simulations and observations for regional health impact assessment. *J. Environ. Res. Public Health*, 16, 2137.